Fundamental studies on deterioration of pharmaceutical humanized IgG - the effect of buffer, contribution of conformational stability and chemical cleavage in heavy chain constant region 2 domain, and detection of deamidated site of IgG -

亀岡, 大介

https://doi.org/10.15017/1560387

出版情報：九州大学, 2015, 博士（創薬科学）, 論文博士
バージョン：
権利関係：全文ファイル公表済

Fundamental studies on deterioration of pharmaceutical humanized IgG − the effect of buffer, contribution of conformational stability and chemical cleavage in heavy chain constant region 2 domain, and detection of deamidated site of IgG –

DAISUKE KAMEOKA

2015

CONTENTS

GENERAL INTRODUCTION

Physiologically active proteins that exist in only small amounts in living organisms can now be produced on an industrial scale by modern biotechnology. Such proteins began being applied as pharmaceuticals from the end of the 1980s, and products from that era, such as erythropoietin and interferon, are utilized as first–generation biopharmaceuticals for a wide range of illnesses. Since the middle of the 1990s, as a result of the development of genomic drug discovery research and molecular investigation of diseases, many disease–related genes and molecules have been discovered. It is expected that substances that specifically inhibit the activity of these disease–related molecules will have a selective and highly therapeutic effect.

Immunoglobulin G (IgG), which is a protein with molecular weight of about 150 kDa, has an interesting feature in that this molecule only interacts with its antigen with high specificity and affinity. IgG thus makes it possible to satisfy the desired goal of a high medicinal effect with few side effects. Theoretically, IgG can be prepared to recognize any target molecule (antigen), and can act on various medical targets. Moreover, because of advances in genetic engineering technology and manufacturing techniques, IgG can be produced on an industrial scale by recombinant cell culture. Therefore, attention is now focused on the application of monoclonal IgG against disease–associated molecules as the second generation of biopharmaceuticals to utilize research on disease–associated genes.

Several types of monoclonal IgG have been developed for medicinal use; these can be classified into murine IgG, chimeric IgG, humanized IgG, and fully human IgG [1]. In general, the effect of murine IgG becomes weaker with long–term dosing, because murine IgG is recognized as a substance foreign to humans and allergic sensitivity occurs. Therefore, to improve safety, investigations have been carried out into designing similar molecules but with human rather than murine IgG, for instance by using genetic engineering technology that introduces the gene expressing human IgG into mammalian cells. As a result, chimeric and humanized types of IgG

have been established and are utilized as pharmaceuticals. Technology that can produce fully human IgG against several different types of antigens is also currently being put into practical use to produce medicinal products [2].

In the case of proteins used as pharmaceuticals, suppressing deterioration during manufacture and preservation is important issue. Regarding IgG for medicinal use, it is necessary to administer doses as high as several grams per kilogram of body weight to achieve beneficial effects. Moreover, to address the needs of patients, the call for subcutaneously injectable formulations is increasing. In order to develop IgG formulations suitable for subcutaneous injection, higher concentrations of IgG in the order of several tens of milligrams per milliliter up to a hundred milligrams per milliliter will be required [3]. At such high concentrations, aggregation of the IgG is expected to be a critical quality attribute because of the high density of the molecules. When proteins used as pharmaceuticals, aggregate arises critical problems. Not only is the pharmacological activity decreased but immunogenicity arises due to the formation of antibodies against the administered protein itself [4]. Therefore, to develop IgG as a medicinal product, conditions of the base solution need to be established such that both the deterioration of the IgG and its aggregation are inhibited.

IgG is a multi–domain protein that unfolds gradually through several steps as the denaturation of each domain. The unfolded IgG intermediates tend to aggregate as a result of the increasing hydrophobicity (Fig. 1). To maintain the activity of the antibody, it is indispensable not only for chemical modification to be inhibited but also for the native higher–order structure to be retained.

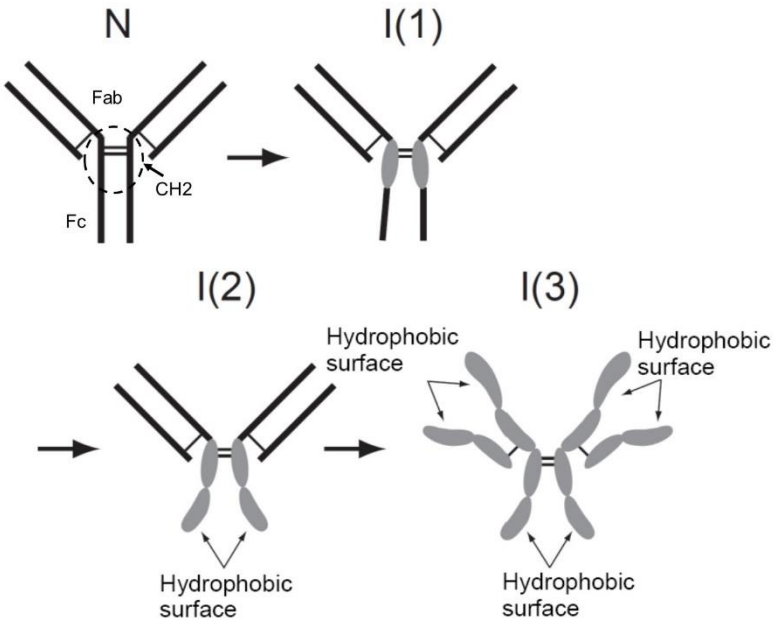

Fig. 1 Schematic representation of the thermal unfolding process of humanized IgG and structural image of each intermediate.

To solve these issues for pertaining the activity of IgG in solution, I performed a series of investigations aimed at developing stable formulations of humanized IgG. I also carried out an attempt to understand which domains of IgG most deeply contributed to aggregation and chemical modification, aiming to establish a more stable molecular platform of IgG.

In the investigation presented in Chapter I, I evaluated the aggregation propensity and structural stability of humanized IgG after heat treatment in the presence of six buffer species. Techniques used included size exclusion chromatography coupled with high–performance liquid chromatography (SEC–HPLC), sodium dodecyl sulfate polyacrylamide gel electrophoresis (SDS–PAGE), and differential scanning calorimetry (DSC). In addition, the domain of the molecule that contributed to the stability of whole IgG molecule was identified by evaluation of stability in the individual Fab and Fc fragments.

In the investigation presented in Chapter II, I evaluated the effect that solution pH had on aggregation propensity in phosphate and 2–(*N*–morpholino)ethanesulfonate (MES) buffers which showed different tendencies with respect to IgG stability. In addition, the contribution of structural

stability in IgG molecule to aggregation was confirmed by using DSC to examine the unfolding temperature of each domain.

In the investigation presented in Chapter III, I evaluated the effect that solution pH had on deterioration using the same buffers as in Chapter II. Based on reduced SDS–PAGE and Edman degradation techniques, I confirmed that cleavage of the Asp–Pro peptide bond in the heavy chain constant region 2 domain (C_H2) domain occurred under acidic conditions. Furthermore, the cleavage rate of IgG monomer and the cleavage rate of a peptide containing the same Asp–Pro sequence were compared to show the contribution of conformational stability of the C_H2 domain to deterioration.

In the study presented in Chapter IV, I investigated the use of matrix–assisted laser desorption/ionization time–of–flight (MALDI/TOF)–mass spectrometry using hen egg–white lysozyme as a model protein to develop an analytical method for identifying chemical modifications, such as deamidation of Asn residues and isomerization of Asp residues, which are critical quality attributes of IgG. Although there were issues in applying MALDI/TOF–mass spectrometry in that these chemical modifications altered the molecular weight of IgG very slightly, I solved this issue by two techniques that involved using endoproteinase Asp–N and ^{15}N–labeled IgG as the standard substance.

ABBREVATIONS

ANS: 8–anilino–1–naphthalene sulfonate

AUC: analytical ultracentrifugation

CD: circular dichroism

CHO: Chinese hamster ovary

DSC: differential scanning calorimetry

EDTA: ethylenediaminetetraacetic acid

FcRn: neonatal Fc receptor

H chains: heavy chains

IgG: immunoglobulin G

IL–6: interleukin–6

L chains: light chains

mAb: monoclonal antibody

MALDI/TOF: matrix–assisted laser desorption/ionization time–of–flight

MES: 2–(*N*–morpholino)ethanesulfonate

MOPS: 3–(*N*–morpholino)propanesulfonate

NMR: nuclear magnetic resonance

PrP: prion protein

PVDF: polyvinylidene fluoride

rhLT: recombinant human lymphotoxin

RP–HPLC: reverse–phase high–performance liquid chromatography

SDS–PAGE: sodium dodecyl sulfate polyacrylamide gel electrophoresis

SEC–HPLC: size exclusion chromatography coupled with high–performance liquid chromatography

CHAPTER I

Effect of Buffer Species on the Unfolding and the Aggregation of Humanized IgG

Abstract

In this chapter, I evaluated the aggregation propensity of humanized antibody after heat treatment in the presence of six buffer species. The comparison under equivalent pH showed high aggregation propensity on phosphate and citrate buffer. In contrast, MES, 3–(*N*–morpholino)propanesulfonate (MOPS), acetate, and imidazole buffer showed lower aggregation propensity than the above two buffers. Meanwhile, unfolding temperature evaluated by differential scanning calorimetry measurement was not altered among these buffer species. The light scattering analysis suggested that heat–denatured intermediate was aggregated slightly on MES and acetate buffer. Therefore, I found that the different aggregation propensity among buffer species was caused from the aggregation propensity of heat–denatured intermediate rather than the unfolding temperature. Furthermore, I revealed that the aggregation dependency on buffer species was accounted for by the specific molecular interaction between buffer and IgG, rather than the ionic strength. On the contrary, on the analyses of unfolding and aggregation propensity by molecular dissection of IgG into Fab and Fc fragments, aggregation propensity of Fc fragment on MES, acetate, and phosphate buffer was almost the same as whole IgG. These findings suggested that the specific interaction between buffer molecule and Fc domain of IgG was involved in the aggregation propensity of heat–denatured IgG.

Introduction

Progress in gene recombinant technology has enabled the large–scale production of many physiologically active proteins that exist in minute concentrations in the living mammalian body, which, in turn, has allowed many physiologically active protein species, such as cytokines and hormones, to be developed into pharmaceutical products. Moreover, treatment with antibodies, which specifically bind to antigen molecules resulting in the so–called antigen–antibody reaction, is of great interest, because many disease–related molecules are being discovered with continuing progress in genome–based drug discovery research. In other words, the application of antibodies specifically directed against disease–related molecules as pharmaceutical products can yield specific therapeutic effects without side effects. Many antibodies developed as pharmaceuticals are currently in use for the treatment of some intractable diseases, such as cancer and rheumatoid arthritis.

For the development of such proteins as described earlier as pharmaceuticals, establishment of a suitable manufacturing process and storage conditions is important to keep the physicochemical properties and the stability of the molecules to be maintained. Unlike the case of the general low–molecular weight pharmaceuticals, not only prevention of deterioration, but also maintenance of the higher–order structure in the native state is necessary to maintain the biological activity of these protein pharmaceuticals. That is, the protein activity can be lost even by partial denaturation occurring near the active center, irrespective of any changes occurring in the primary structure. Therefore, most proteins must be protected against denaturation occurring during storage. On the other hand, aggregation can cause serious problems in quality control, especially for liquid formulations of the protein drug substances [5, 6]. In general, aggregated proteins are insolubilized with the growth of the molecular size, causing the formation of insoluble particles in the protein formulation. Even if such insoluble particles are not formed, aggregation of proteins causes a loss of the biological activity [7]. Moreover, administration of such aggregated protein products could

cause some critical immune reaction–related adverse effects, including anaphylactic shock. In the meantime, the solution conditions, such as the pH and the salt species and concentration, can alter the physicochemical properties from the viewpoint of aggregation and chemical modification, of proteins and reduce the protein stability. For example, recombinant factor VIII SQ is stable only in a narrow range of solution pH that is, 6.5–7.0, and its aggregation is inhibited in the presence of high concentrations of sodium chloride in the solution [8]. Therefore, establishment of optimal solution conditions is important for suppressing chemical modification so as to maintain the protein stability and retain the higher–order structure.

IgG is a protein molecule with a molecular weight of about 150 kDa, and is composed of two heavy chains (H chains) and two light chains (L chains) connected by disulfide bonds and non–covalent interactions. This molecule also has the features of multi–domain proteins, and consists of two Fab domains and one Fc domain, and a secondary structure with a high content of β–sheets. Aggregation of IgGs in high–concentration solutions poses some serious problems in their pharmaceutical application because the administration dose of IgGs is usually more than 100 mg/kg–bodyweight, and the IgG concentrations in drug products become rather high, often in the order of several tens of mg/mL. The influence of heat treatment and pH on the denaturation and aggregation of IgGs in solution has been a subject of investigation for a long time. However, there have been few reports on the systematic research of denaturation and aggregation using humanized monoclonal antibody (mAb). Therefore, the optimal solution conditions under which the formation of aggregates or denatured intermediates of IgG can be suppressed need to be investigated. On the other hand, the thermodynamic properties of immunoglobulins have been examined in detail using DSC. There are two or more transitions during their heat denaturation phenomenon, and it has been reported that these transitions are attributable to denaturation of each of the unit domains [9, 10]. Recently, Ejima et al. analyzed the effect of pH on the conformation, stability, and aggregation of humanized mAbs (hIgG4–A, –B) using circular dichroism (CD), DSC, and sedimentation

velocity [11]. Therefore, DSC analyses of IgG or its fragments may be useful to investigate the mechanism of unfolding and aggregation of IgG.

In this chapter, I analyzed the heat–denatured aggregation of humanized whole antibody and its fragments in the presence of several buffer species, in order to know the optimal condition where humanized IgG was stable and the mechanism of heat–denatured aggregation of humanized IgG.

Materials and Methods

Materials and reagents

The immunoglobulin (IgG), a humanized mAb specific for the human interleukin–6 (IL–6) receptor, was donated by Chugai Pharmaceuticals (Tokyo, Japan). TSK–gel G4000SWXL column (7.8 × 300 mm) was purchased from Tosoh (Tokyo, Japan), and the HiTrap Protein A HP column was obtained from Amersham Biosciences (Piscataway, USA). All other chemicals were of analytical grade for biochemical use.

Preparation of the samples of whole IgG and the IgG fragments

Sample solutions of whole IgG at a concentration of 10 mg/mL (66.7 μM), differing in pH and containing different buffer species were evaluated in this study. I used the buffer species phosphate, citrate, imidazole, MES, and MOPS at pH 6.5 and phosphate, citrate, acetate, and MES at pH 5.5. The buffer concentration in all the solutions was 15 mM. The solutions were prepared from an IgG stock solution that contained 50 mg/mL of IgG in 15 mM sodium phosphate buffer, pH 6.5, by dialysis and dilution.

Fab and Fc fragments of IgG were obtained by papain digestion at 37°C, and separated on a HiTrap Protein A HP column. The Fab fragments were further purified using a Resource S column by cation exchange separation. Sample solutions of the Fab and Fc fragments (1 mg/mL) dissolved

in various buffer solutions were prepared by dialysis and dilution. In this case, I used the buffer species phosphate, citrate, and MES at pH 6.5, and phosphate, citrate, and MES at pH 5.5.

Assessment of stability of the IgG sample solution

In order to evaluate the stability of the whole IgG and the IgG fragments in solution, the sample solutions were subjected to heat treatment at 60°C for 4 weeks. In the case of the whole IgG solutions, additional heat treatment at 80°C for 2 h was also performed.

The percentages of the residual monomer IgG and of the soluble aggregates formed were evaluated by SEC–HPLC. The percentages of residual IgG fragments were also measured by the same method. Untreated and heat–treated sample solutions were diluted with water to 1 mg/mL and applied to a HPLC system (Waters) with a TSK–gel G4000SWXL column and eluted with 50 mM phosphate buffer, pH 7.0, containing 0.3 M NaCl.

The purity of the whole IgG was evaluated by SDS–PAGE [12]. Untreated and heat–treated sample solutions, either with or without 2–mercaptoethanol, were diluted with 10% SDS–containing buffer to obtain a final protein concentration of 100 mg/mL. Samples containing 2–mercaptoethanol were boiled for 5 min for reducing the IgG, and then applied to a 12% polyacrylamide gel under reducing conditions or 8% polyacrylamide gel under non–reducing conditions and electrophoresed at 200 mA for about 40 min. Protein bands were stained with Coomassie brilliant blue.

Furthermore, 8–anilino–1–naphthalene sulfonate (ANS) binding was measured to evaluate the surface hydrophobicity of the IgG fragments. ANS solution (0.4 mM) was added to each diluted heat–treated or untreated sample solution to obtain a final molar ratio of ANS to each IgG fragment of 10. The fluorescence spectra of the ANS solutions between 450 and 550 nm after excitation at 365 nm were measured at room temperature using an F–2000 fluorescence spectrophotometer (Hitachi, Tokyo, Japan).

Differential scanning calorimetry

The DSC measurements were carried out using a VP–DSC calorimeter (MicroCal). Each sample solution of whole IgG, Fab or Fc fragment was diluted to 0.5 mg/mL with the same buffer solution without IgG. DSC scans were performed at a rate of 0.5°C/min in the temperature range of 40–105°C. Data were analyzed using the Origin software (MicroCal).

Aggregation of the heat–denatured intermediates

Rayleigh scattering of the heat–denatured intermediates was monitored to evaluate their aggregation propensity. The heat–denatured intermediate stock solution with an IgG concentration of 10 mg/mL dissolved in 5 mM MES buffer, pH 5.5, was prepared by heat treatment of the IgG solution, by gradually raising the temperature from 40°C to 90°C at the rate of 0.17°C/min. Then, denatured IgG stock solution was added to the buffer solutions without IgG to adjust the IgG concentration to 500 mg/mL. The buffer species used in this experiment were phosphate (pH 5.5 and 6.5), citrate (pH 5.5), acetate (pH 5.5), and MES (pH 5.5 and 6.5). After the addition of denatured IgG, the Rayleigh scattering intensity of each buffer solution was monitored at 340 nm by an RF–5300 fluorescence spectrophotometer (Shimadzu, Kyoto, Japan) at room temperature.

Effect of the ionic strength of the solution on the aggregation of whole IgG

The IgG solutions with various buffer species with differing ionic strengths, with ratios of 0.001, 0.01, and 0.1, were prepared by the dialysis to each buffer. I used phosphate (pH 5.5 and 6.5), citrate (pH 5.5), acetate (pH 5.5), and MES (pH 5.5 and 6.5) as the buffer species. The IgG concentration of each solution was 10 mg/mL. Then, the percentage of the residual IgG monomer after heat treatment at 60°C for 4 weeks was evaluated by SEC–HPLC, as described earlier.

Results

Aggregation of the whole IgG after heat treatment

The propensity to aggregation of the humanized IgG after heat treatment at 80°C for 2 h and 60°C for 4 weeks was evaluated in solutions containing each of the six buffer species at a constant molar concentration, by SEC–HPLC and SDS–PAGE. The typical SEC–HPLC chromatograms of the IgG solutions before and after heat treatment showed aggregation of most of the IgG monomers by the heat treatment (Fig. I–1). The percentages of the residual monomer and the aggregates of IgG after heat treatment in solutions containing each of the buffer species are shown in Table I–1. After the heat treatment at 80°C for 2 h, percentage of residual monomer differed markedly among buffer species. In particular, MES buffer on pH 5.5 showed quite high residual monomer of 75%. In addition, MES, MOPS and imidazole buffers at pH 6.5 showed relatively high residual monomer of the range from 50% to 60%. Citrate and phosphate buffers on both pH showed low percentage of residual monomer. On the contrary, after the heat treatment at 60°C for 4 weeks, marked percentage difference of residual monomer was not found among buffer species except for MES buffer at pH 5.5 which showed high residual monomer of 72%. However, total percentage of residual monomer and aggregate fell much below 100% in phosphate and citrate buffers at pH 6.5, because insoluble aggregate was formed in IgG solutions with such a condition. In other buffer species, such insoluble aggregate was not detected.

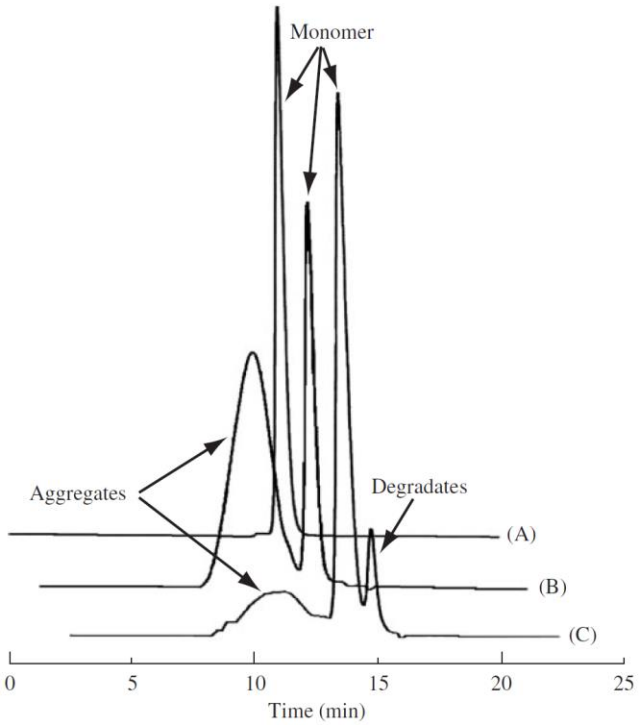

Fig. I–1 Size exclusion chromatograms of humanized IgG in 15 mM phosphate buffer, pH 6.5 before and after heat treatment. (A) Before heat treatment, (B) After 80°C storage for 2 h, (C) After 60°C storage for 4 weeks.

Table I–1 Percentages of the residual monomer and the soluble aggregates in humanized IgG solution containing different buffer species after heat treatment

Buffer species		80°C–2 h		60°C–4 weeks	
		Monomer (%) [a]	Aggregates (%) [a]	Monomer (%) [a]	Aggregates (%) [a]
Phosphate	pH 6.5	28.3	68.1	49.4	8.3 [b]
Citrate	pH 6.5	22.5	63.4	54.1	14.9 [b]
Imidazole	pH 6.5	60.6	31.7	60.0	25.5
MES	pH 6.5	53.2	44.4	59.7	31.0
MOPS	pH 6.5	51.9	39.0	58.7	31.5
Phosphate	pH 5.5	49.1	48.9	47.1	43.2
Citrate	pH 5.5	21.4	75.3	21.4	65.0
Acetate	pH 5.5	58.7	36.8	58.7	32.8
MES	pH 5.5	75.4	9.9	72.1	16.0

[a] Percentages of the monomer and the aggregate content was the ratio of the peak area after heat treatment to the monomer peak area before heat treatment

[b] Insoluble aggregates were formed after heat treatment at 60°C for 4 weeks.

In order to confirm the presence or absence of covalent bonds in the aggregates, the IgG solutions was subjected to non–reduced and reduced SDS–PAGE after heat treatment at 80°C for 2 h and at 60°C for 4 weeks. The electropherograms of IgG solutions in phosphate buffer at pH 5.5 and MES buffer at pH 5.5 after heat treatment at 80°C for 2 h are shown in Fig. I–2 as typical results of buffers with different stability. Some bands, corresponding to the aggregates, were detected in the higher molecular weight range than monomers by SDS–PAGE under non–reducing conditions. However, the proportion of the aggregates as calculated from the band intensity was lower than that calculated by SEC–HPLC. On the other hand, the band distribution in the SDS–PAGE under reducing conditions was not changed by heat treatment. Next, the electropherograms of IgG solutions in phosphate buffer at pH 5.5 and MES buffer at pH 5.5 after heat treatment at 60°C for 4 weeks are shown in Fig. I–3 and the results are similar to those obtained following heat treatment at 80°C for 2 h. In this figure, not only the significant band corresponding to the aggregates seen in the electropherograms of SDS–PAGE under non–reducing conditions, but also the band in a higher molecular weight range than that corresponding to the H chain seen in those of SDS–PAGE under reducing conditions was observed. Therefore, most of the increase of the aggregates observed after heat treatment at 80°C storage represented the non–covalent species, whereas some covalent aggregates formed by inter–chain disulfide bonding. On the other hand, the aggregates formed after heat treatment at 60°C were shown to be cross–linked by various covalent bonds, including inter–chain disulfide bonds. In addition, the bands corresponding to the aggregates in phosphate and citrate buffers showed relatively high intensity, irrespective of the heat treatment condition.

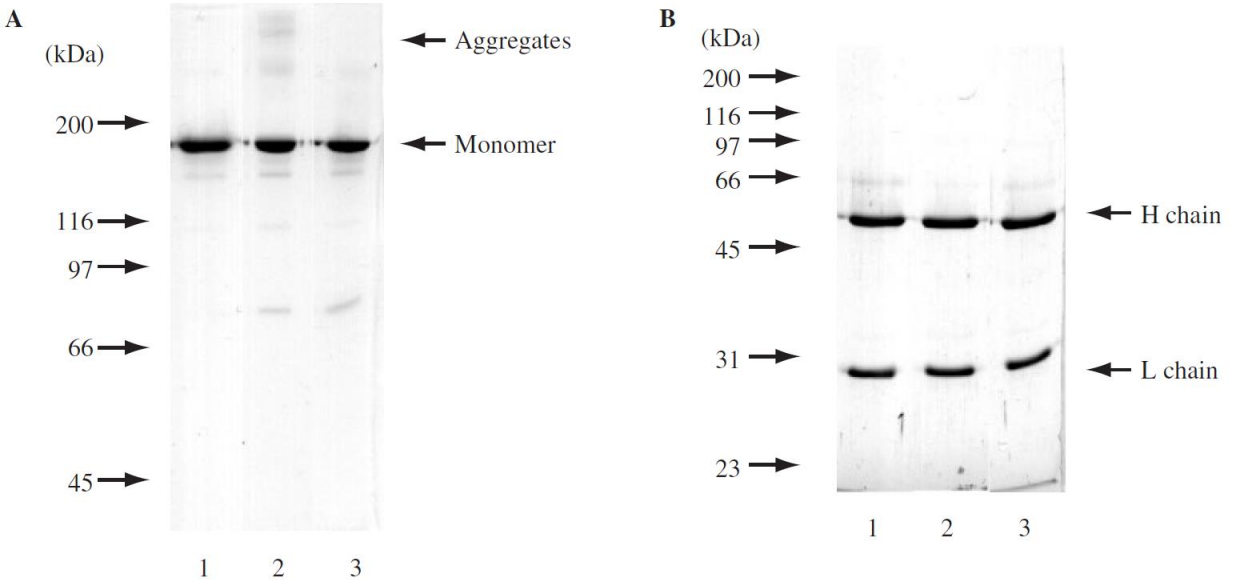

Fig. I–2 Non–reduced (A) and reduced (B) SDS–PAGE analysis of humanized IgG before and after 80°C storage for 2 h. Lane 1: Before storage in 15 mM phosphate buffer, pH 5.5; Lane 2: After 80°C storage in 15 mM phosphate buffer, pH5.5; Lane 3: After 80°C storage in 15 mM MES buffer, pH 5.5.

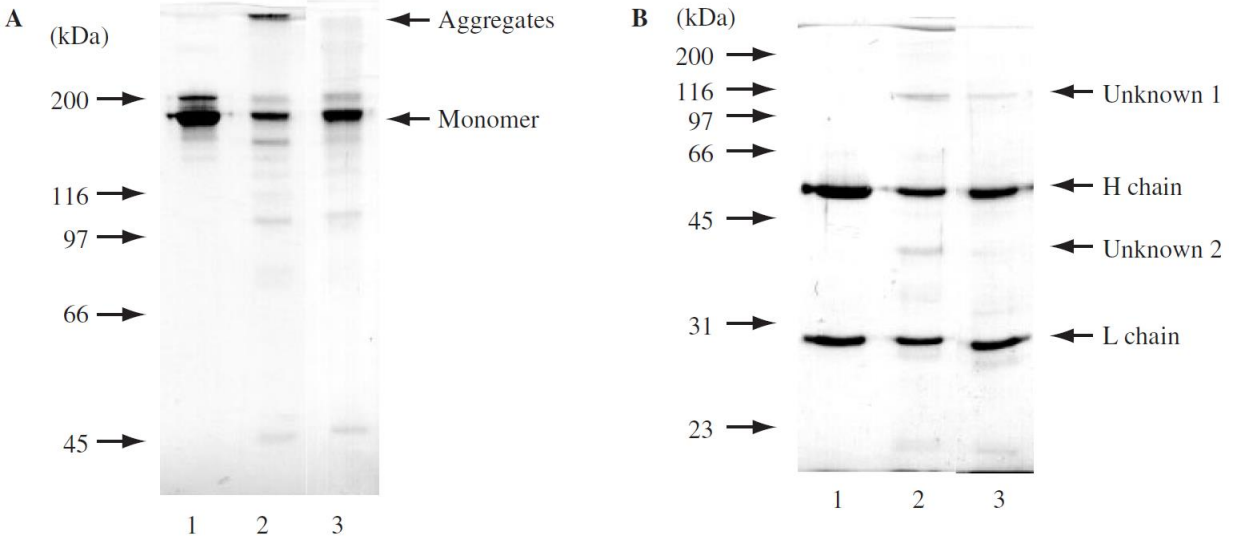

Fig. I–3 Non–reduced (A) and reduced (B) SDS–PAGE analysis of humanized IgG before and after 60°C storage for 4 weeks. Lane 1: Before storage in 15 mM phosphate buffer, pH 5.5; Lane 2: After 60°C storage in 15 mM phosphate buffer, pH 5.5; Lane 3: After 60°C storage in 15 mM MES buffer, pH 5.5.

Evaluation of the unfolding temperature by DSC

Direct scanning calorimetry of the antibody solutions was performed to evaluate the unfolding temperature of the IgG in solutions containing each of the five buffer species. The DSC thermograms and the unfolding temperatures determined are shown in Fig. I–4 and Table I–2, respectively. These results suggest that heat denaturation of this IgG occurred in three steps, that is, unfolding of the Fc domain corresponding to the first two endothermic peaks, and that of the Fab domain corresponding to the last endothermic peak. However, the unfolding temperature of each buffer species with any of the unfolding steps did not correlate with the difference of aggregation propensity. In contrast, because of the appearance of an exothermic signal during the third unfolding step, the corresponding unfolding temperature could not be measured in the phosphate and citrate buffer solutions. This phenomenon was thought to be attributable to convection in the DSC cell due to protein aggregation, therefore it was suggested that the IgG aggregation occurred during the third unfolding step. In fact, sample solution of these buffer solutions recovered from DSC cell was clouded.

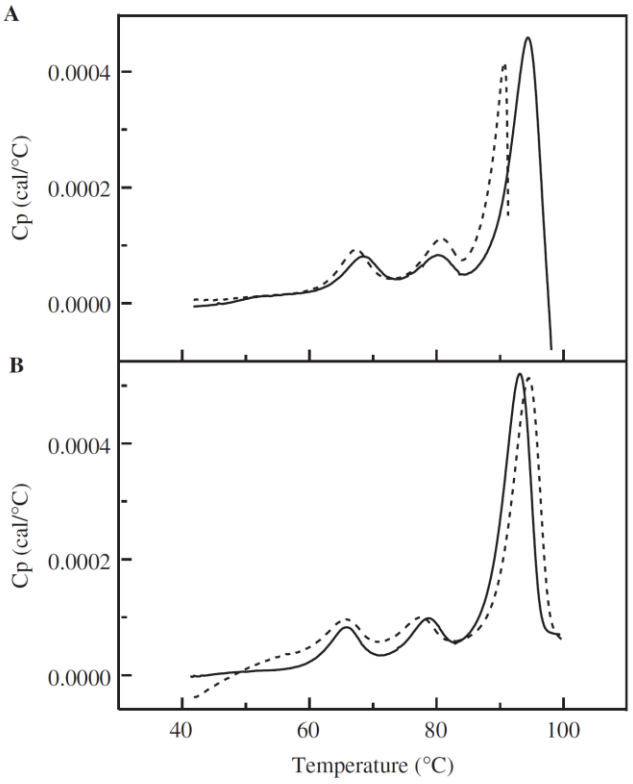

Fig. I–4 DSC thermograms of humanized IgG in different buffer species. (A) Group H buffers: 15 mM phosphate buffer, pH 5.5 (solid line) and 15 mM citrate buffer, pH 5.5 (dotted line). (B) Group L buffers: 15 mM MES buffer, pH 5.5 (solid line) and 15 mM acetate buffer, pH 5.5 (dotted lines). The protein concentration was 0.5 mg/mL.

Table I–2 Unfolding temperatures of whole and each fragments of humanized IgG in different buffer species

Buffer species		Tm [a] (°C)		
		Whole IgG		
		First step	Second step	Third step
Phosphate	pH 6.5	NT [b]	NT [b]	NT [b]
MES	pH 6.5	70.7	79.7	94.3
Imidazole	pH 6.5	67.3	76.3	93.9
Phosphate	pH 5.5	68.6	80.2	94.3 [c]
Citrate	pH 5.5	67.7	81.3	91.5 [c]
Acetate	pH 5.5	65.6	77.5	94.4
MES	pH 5.5	66.5	79.2	93.6

Buffer species		Tm [a] (°C)		
		Fc		Fab
		First step	Second step	
Phosphate	pH 6.5	70.3	— [d]	92.9
MES	pH 6.5	69.8	— [d]	94.3
Imidazole	pH 6.5	NT	NT	NT
Phosphate	pH 5.5	NT	NT	NT
Citrate	pH 5.5	67.0	— [d]	93.1
Acetate	pH 5.5	68.8	81.1	94.3
MES	pH 5.5	66.5	80.8	93.6

[a] Tm was defined as the peak top of IgG or its fragments during thermal unfolding

[b] NT: Not tested

[c] Whole IgG was aggregated during the third denaturation step

[d] Fc fragment was aggregated during the second denaturation step

Aggregation of the heat–denatured intermediate

The light scattering intensity of each buffer species after addition of the non–aggregated heat–denatured intermediate was measured to evaluate the aggregation propensity of the intermediate. The time–courses of the changes in the Rayleigh light scattering intensity at 340 nm in the phosphate, citrate, acetate, and MES buffer solutions are shown in Fig. I–5. A light scattering

intensity after the addition of heat–denatured intermediate was not altered in MES and acetate buffers. On the contrary, this light scattering intensity was increased in phosphate and citrate buffers, and the rate of increase was in the order of citrate pH 6.5 > phosphate pH 6.5 = citrate pH 5.5.

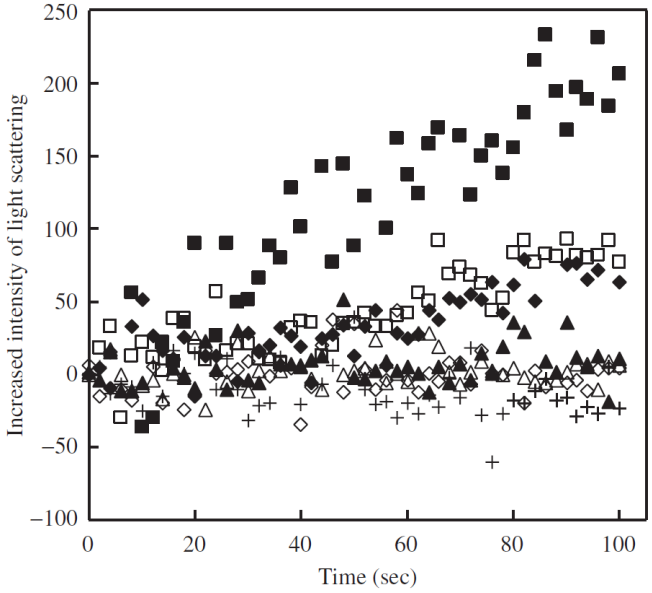

Fig. I–5 Time courses of the light scattering intensity at 340 nm after the heat–denatured intermediate addition in different buffer species: 15 mM phosphate buffer, pH 6.5 (closed diamonds) and 5.5 (open diamonds); 15 mM citrate buffer, pH 6.5 (closed squares) and 5.5 (open squares); 15 mM MES buffer, pH 6.5 (closed triangles) and 5.5 (open triangles); and 15 mM acetate buffers, pH 5.5 (crosses).

Effect of the ionic strength of the solution on the aggregation of whole IgG

In order to evaluate the effect of the ionic strength of the solution on the IgG aggregation, IgG solutions with a similar ionic strength of the buffer species were stored at 60°C for 4 weeks. The percentages of the aggregates after heat treatment in the phosphate, citrate, acetate, and MES buffer solutions are shown in Fig. I–6. The percentages of the aggregates increased with increasing ionic strength for all the buffer species. Correspondingly, the percentage of residual monomer after heat treatment decreased with increasing percentage of the aggregates. On the other hand, the percentage of the aggregates did not differ among the different buffer species (phosphate, acetate, and MES) having an equal ionic strength. Interestingly, the percentage of residual monomer was relatively high even at a high ionic strength of the MES buffer, pH 6.5. Also, the percentage of aggregates formed in the citrate buffer was higher than that in the phosphate, acetate, and MES buffers, even for an equal ionic strength.

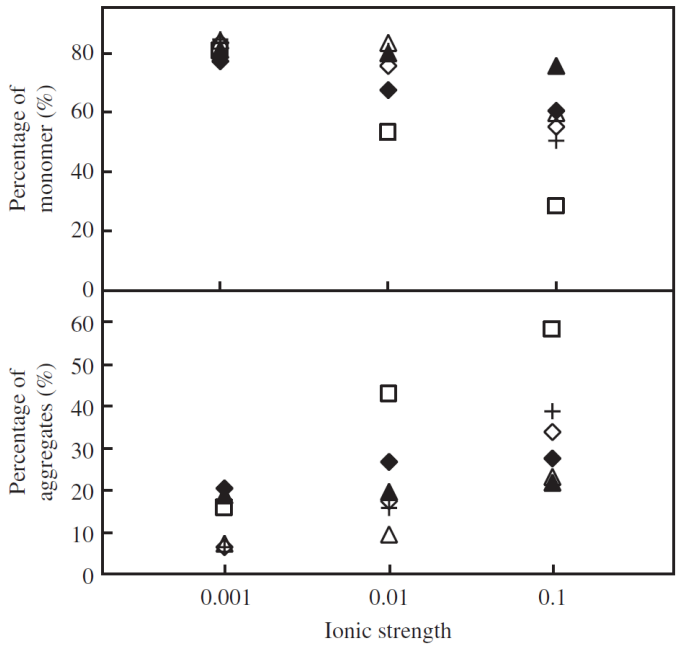

Fig. I–6 Effect of ionic strength on the aggregation of humanized IgG in different buffer species: 15 mM phosphate buffer, pH 6.5 (closed diamonds) and 5.5 (open diamonds); 15 mM citrate buffer, pH 5.5 (open squares); 15 mM MES buffer, pH 6.5 (closed triangles) and 5.5 (open triangles); 15 mM acetate buffers, pH 5.5 (crosses).

Thermal stability of the Fab and Fc domains

The effect of the buffer species on the thermal stability of the Fab and Fc fragments prepared by papain digestion of IgG was evaluated after heat treatment at 60°C. The percentage of the residual monomer and the ANS protein binding fluorescence of the Fab and Fc fragments in phosphate, citrate, acetate, and MES buffer solutions after heat treatment at 60°C are shown in Table I–3. The percentage of the Fab fragment monomer after storage at 60°C for 4 weeks was almost 100% in all the buffer species, except citrate. In addition, no ANS protein binding was detected in any of the buffer species because fluorescence intensity was not increased after ANS addition. On the other hand, the percentage of the residual Fc fragment monomer was decreased to 50–70% even after storage at 60°C for 1 week, without any significant differences among the buffer species. Furthermore, the ANS protein binding fluorescence was increased in the Fc fragment solutions, and the maximum increase was observed in the solution in citrate buffer, pH 5.5.

Table I–3 Percentage of each residual fragment and increase of ANS fluorescence intensity [a] in the solutions of humanized IgG fragments containing different buffer species after heat treatment

Buffer species		Fab (60°C–4weeks)		Fc (60°C–7days)	
		Residual (%)	Increase of ANS fluorescence	Residual (%)	Increase of ANS fluorescence
Phosphate	pH 6.5	94.1	25	65.1	311
Citrate	pH 5.5	67.9	–20	55.6	1365
MES	pH 6.5	93.4	8	62.5	137
MES	pH 5.5	99.8	7	51.1	532
Acetate	pH 5.5	90.5	0	68.6	246

[a] ANS fluorescence intensity was monitored at 470 nm after excitation at 365 nm

The DSC thermograms and the determined unfolding temperature of each IgG fragment in each of the buffer species are shown in Fig. I–7 and Table I–2, respectively. The Fab fragment solution showed an endothermic peak corresponding to the third unfolding step of whole IgG, and the unfolding temperature determined was 94°C, irrespective of the buffer species used. On the other hand, the Fc fragment solutions showed two endothermic peaks corresponding to first and second unfolding steps of whole IgG. While the first unfolding temperature of the Fc fragment was 67–70°C, irrespective of the buffer species used, the second unfolding temperature of the Fc fragment differed significantly among the buffer species, and a dramatic exothermic signal appeared in all except the MES buffer, pH 5.5, possibly due to the aggregation propensity of the partially unfolded molecule. The signal of the second unfolding step was, however, especially difficult to confirm in the phosphate and citrate buffer solutions.

Discussion

Effect of buffers on the aggregation of IgG

Because of the restricted pH range in which high protein stability can be maintained, the pH of protein solutions should be controlled precisely within the appropriate range for each molecule to maintain the protein stability and prevent protein aggregation. Therefore, buffer solutions are employed in many cases for long–term protein storage. To determine the most suitable buffer species for each protein solution, the effects of the buffer species on the protein stability should be evaluated. In this chapter, the influence of six buffer species on the aggregation of humanized IgG was evaluated. As a result, low aggregation propensity in MES, MOPS, and imidazole buffers and high aggregation propensity in phosphate and citrate buffers were found (Table I–1). Therefore, for humanized IgG, it was suggested that the buffer containing morpholine, sulfonic acid, and imidazole retarded the formation of heat–denatured intermediates. So, in order to know which functional groups retard the formation of heat–denatured intermediates, further study will be necessary using the other types of buffers. And also, the possibilities to extrapolate the effect of buffer species on the inhibition of protein aggregation for other proteins need to be investigated.

Involvement of heat–denatured intermediate on aggregation of IgG

Since no differences in the unfolding temperature were observed among several buffer solutions in this chapter, the DSC results could not be attributed to differences in the aggregation propensity of IgG (Table I–2). However, the exothermic signal due to aggregate formation during the 3rd unfolding step was detected only for phosphate and citrate buffer solutions which showed high aggregation propensity (Fig. I–4). From these findings, it was suggested that the differences in the IgG aggregation propensity among buffer species were considered to be attributable to aggregation of the heat–denatured intermediate.

The aggregation mechanism of many proteins can be expressed as a two–step reaction consisting of denaturation and aggregation processes [13]. One is the reversible process from native state to intermediate state, and the other is the irreversible process from the intermediate to aggregation state. This supposition implies that the aggregation propensity is closely related to the heat–denatured intermediates. The present results were consistent with the previous idea [13] because the light scattering intensity was increased in phosphate and citrate buffer solutions, where the heat–denatured intermediate was observed (Fig. I–5). From the above results, IgG aggregation was affected by the stability of the heat–denatured intermediate rather than the unfolding temperature. Therefore, the suppressed aggregation of humanized IgG in these stable buffer solutions such as MES and acetate was considered to be attributable to the higher stability of the hydrophobic heat–denatured intermediate with a low aggregation propensity. In fact, the aggregation of ABX–IL8 antibody, as measured by DSC, was inhibited in histidine buffer containing an imidazole group [14]. Since the finding for ABX–IL8 antibody was consistent with the present results, the information obtained from this study can generally be applied to many other humanized antibodies, especially subtype IgG1 antibodies.

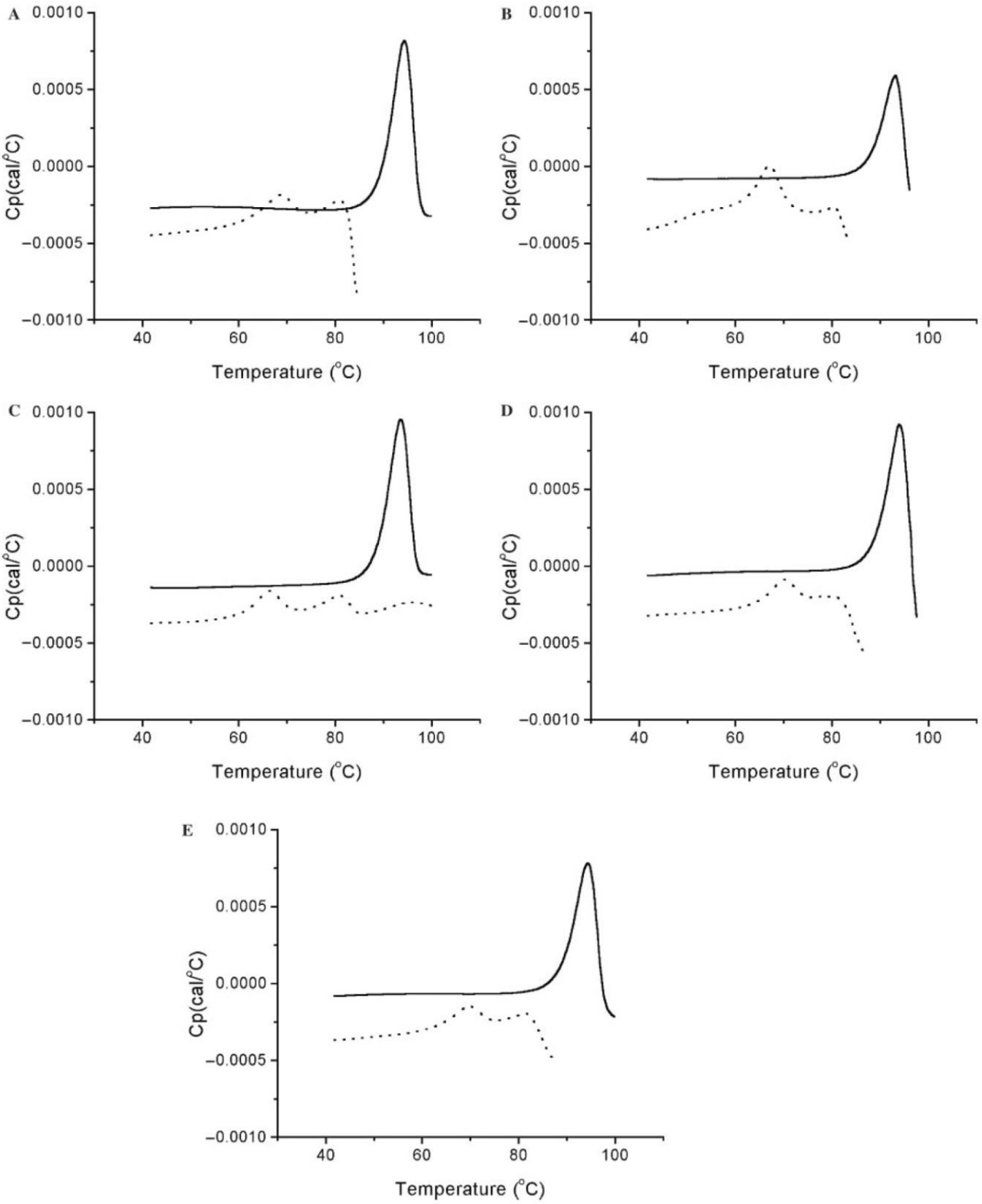

Fig. I–7 DSC thermogram of each humanized IgG fragments in different buffer species.

(A) 15 mM acetate buffer, pH 5.5; (B) 15 mM citrate buffer, pH 5.5; (C) 15 mM MES buffer, pH 5.5; (D) 15 mM MES buffer, pH 6.5; (E) 15 mM phosphate buffer, pH 6.5. Solid line, Fab fragment; dotted line, Fc fragment. The protein concentration was 0.5 mg/mL.

Contribution of ionic strength of buffer for the aggregation of IgG

In this chapter, the effects of the buffer species on the aggregation of humanized IgG were compared under the condition of a constant molar concentration. However, the effects may originate from differences in the ionic strength, because the ionic charges were different among the various buffer species. In fact, evaluation of the influence of the ionic strength on the aggregation propensity after heat treatment showed that the percentage of aggregates in all the buffer species increased in proportion to the ionic strength (Fig. I–6). In addition, the aggregation propensity was not different in the equal ionic strength, except for the case of citrate buffer. Generally, the hydrophobic interaction could represent the main intermolecular interaction under high ionic strength conditions after salt addition, because the electrostatic repulsion due to the negative charge on this molecule could be weakened. Therefore, the acceleration of protein aggregation under high ionic strength conditions observed in this chapter may imply that the hydrophobic interaction could be the dominant factor for aggregation. In other words, the higher aggregation propensity of humanized IgG in phosphate buffer as compared with that in the other buffer species containing equal buffer concentration could only be due to the higher ionic strength of phosphate buffer. On the other hand, the aggregation propensity in all the buffer species cannot be explained by only differences in the ionic strength. For example, MES buffer specifically inhibited the aggregation of humanized IgG at pH 6.5, but citrate buffer accelerated such aggregation under both the pH conditions examined, despite the equal ionic strength. From these results, it was suggested that some interaction of the buffer ions with the protein surface stabilized or destabilized the protein itself. This proposition is interesting from the viewpoint of resolving the effects of the buffer species on protein aggregation, and could be clarified from identification of the binding positions of the buffer ions on the protein surface. For example, comparative evaluation of the suppression of IL–1ra aggregation in high concentration solutions of three anion species showed the lowest effect of phosphate ions, perhaps attributable to the low affinity of this anion to its binding site on IL–

1ra [15]. Such knowledge is important to obtain an understanding at the molecular level of suppression mechanism of protein aggregation by buffer species, which has until now been discussed only on an empirical basis.

Aggregation of whole IgG is caused by that of Fc fragment

The heat denaturation process of IgG can be divided into several denaturation steps of the Fc and Fab domains, and both of the denaturation processes occur independently. Vermeer et al. has discussed this thermodynamic fact in detail based on their series of research on isotype 2b IgG [9, 16]. In their studies, the denaturation temperature of the Fab and Fc fragments of the above IgG prepared by papain digestion was comparable to that of whole IgG, and the heat denaturation of whole IgG was able to be expressed as the summation of that of the Fab and Fc domains. Moreover, the denaturation peak detected during DSC of the anti–p24 (HIV–1) mAb CB 4–1 was also assigned to the denaturation of the Fab and Fc domains, and the influence of pH on the denaturation temperature of each was confirmed [17]. Taking into consideration these references, separation of the Fab and Fc fragments is often used to investigate the changes in the physicochemical properties of whole IgG and to discuss the denaturation mechanism of IgG. In this chapter, the influence of buffer species on the aggregation propensity and denaturation temperature of the Fab and Fc fragments prepared by papain digestion was evaluated to clarify which domain might contribute to aggregation of the whole humanized IgG. The results revealed no aggregation of the Fab fragment after heat treatment at 60°C for 4 weeks in any of the buffer species, except citrate, but the aggregation propensity of the Fc fragment depended on the buffer species, as in the case of whole IgG (Table I–3). On the other hand, the results of DSC revealed that the denaturation temperature of both fragments was equal to that of the whole IgG, but an exothermic peak was detected after the denaturation of the Fc fragment as in the case of the whole IgG in all the buffer species, except in the MES buffer at pH 5.5 (Table I–2 and Fig. I–7). From these results, since the aggregation

propensity of the whole IgG and Fc fragment was similar, it was suggested that Fc was the important domain which governed the aggregation of whole IgG.

Adequate buffer solution is effective aggregation inhibitor

Many approaches for suppressing protein aggregation have been attempted to maintain the stability of protein solutions in storage. Addition of stabilizers, such as sugars and amino acids, is a widely used technique for suppressing protein aggregation. Sugars and sugar alcohols are preferentially excluded from the protein surface in the protein solution, and the protein is preferentially hydrated [18]. As the free energy of the native protein is decreased by the preferential hydration, the hydrated protein shows an increase in the denaturation temperature. Moreover, basic amino acids, such as L–arginine suppressed the aggregation and precipitation of the intermediates with high hydrophobicity during the protein refolding process by interacting with the hydrophobic protein surface [19]. Arakawa et al. reported that arginine suppressed aggregation of IL–6 and a mAb concentration–dependently during thermal unfolding [20]. However, in such an approach, extensive additional amounts of the stabilizers are needed, which results in a marked increase in the osmotic pressure of protein solution. Such a high osmotic pressure shows little adequacy for pharmaceutical application, in particular, for subcutaneous injection because isotonicity of administrative solution is effective to reduce the pain on injection. Therefore, additives which can be added in small quantities to suppress protein aggregation are desirable. The results of this study revealed that the aggregation of humanized IgG was able to be inhibited without the addition of large amounts of stabilizers, by adding small concentrations, in the millimolar range, of suitably selected buffer species. Moreover, it was shown that the inhibition of humanized IgG aggregation was due to stabilization of the heat–denatured intermediates. Thus, humanized IgGs can be applied as a pharmaceutical possessing numerous different antigen–binding abilities only by inducing slight structural changes of the antigen–binding site. In conclusion, the method attempted for the

suppression of protein aggregation in this chapter is expected to allow the application of humanized IgGs as pharmaceuticals.

CHAPTER II

Effect of the Conformational Stability of the C_H2 Domain on the Aggregation of a Humanized IgG

Abstract

In Chapter I, I found that the different aggregation propensities seen with different buffer species was due to the aggregation propensities of heat–denatured intermediates rather than to the unfolding temperature. In addition, I suggested that specific interactions between buffer molecules and the Fc domain of IgG were involved in the aggregation propensity of heat–denatured IgG. In this chapter, to reveal the effect of the conformational stability of the C_H2 domain on aggregation, I compared the percentage of residual monomer and the percentage of aggregation of the samples at various pH (4.0–9.0) after incubation at 60°C and 80°C. In this thesis, MES and phosphate were used based on the different aggregation propensities found in Chapter I. I observed differences between the two incubation conditions in terms of the pH dependencies of aggregation. The percentage of residual monomer in the samples incubated at 80°C increased as pH declined, but with long incubation at 60°C the percentage of residual monomer showed a maximum value at pH of 6.0–7.0. That is, aggregation of humanized IgG1 occurred during long incubation at 60°C under acidic conditions. From the DSC measurements, I revealed that this tendency could be attributable to the decrease in unfolding temperature in the first step due to the instability of the C_H2 domain at lower pH and to the increase in aggregation propensity of heat–denatured intermediates at higher pH. In addition, I found that MES inhibited aggregation of IgG1 in the pH ranges of 4.0–5.0 and 7.0–8.0.

Introduction

IgG molecules have two characteristic structural features: they are multi–domain proteins comprising two Fab domains and one Fc domain, and they have rich β–sheet structures. It is reported that the multiple characteristic transitions observed during heat denaturation of IgG molecules are a result of the successive unfolding of each of its domains [9, 10, 21, 22]. The aggregation of IgGs in concentrated solutions is a serious problem for pharmaceutical applications because such applications require high dosages (typically ≥100 mg per body). In Chapter I, I reported the results of a study conducted to search for superior storage conditions for a humanized IgG1 antibody at pH 5.5 or 6.5. I found aggregation was lower in MES, MOPS, acetate, and imidazole buffers than it was in phosphate and citrate buffers.

Acidic conditions are widely used to elute IgG from Protein A affinity columns and to inactivate viruses during the purification of therapeutic antibodies. To clarify IgG aggregation mechanisms, many researchers have studied aggregation under acidic conditions. In one study, for example, it was found that changes in the secondary and tertiary structures contributed to the aggregation of an IgG2 antibody that undergoes marked aggregation at pH 4.0 to 5.0 [23]. In another study, structural changes in two humanized antibodies under acidic conditions were researched in detail by using DSC, CD, and analytical ultracentrifugation (AUC) [11]. Such results suggested that the formation of denatured intermediates, in which hydrophobic surfaces were exposed, contributed to the aggregation of IgG molecules. Therefore, investigation of aggregate formation in various buffer solutions at various pH levels is important in relation to increasing the stability of IgG formulations in a liquid state.

Thus, in this chapter, I evaluated the aggregation of a humanized IgG1 following storage at pH levels ranging from 4.0 to 9.0 in two different buffers by using SEC–HPLC and SDS–PAGE. The first buffer was phosphate, which is widely used in biochemical experiments; the other was MES, which I found in Chapter I to be a superior buffer for storage of humanized IgG1 at pH 5.5 and 6.5.

I also investigated the effect of structural stability on the aggregation of humanized IgG1 by evaluating its unfolding temperature at each pH.

Materials and Methods

Materials and reagents

The IgG molecule investigated in this chapter was the same monoclonal antibody used in Chapter I. The TSK–gel G4000SWXL column (7.8 × 300 mm) used was purchased from Tosoh (Tokyo, Japan).

Preparation of the IgG1 monomer sample solutions

I prepared IgG1 sample solutions from an IgG1 stock solution (50 mg/mL IgG1 in 15 mM sodium phosphate buffer, pH 6.5) by dialysis, pH adjustment, and dilution. The prepared sample solutions contained 10 mg/mL (66.7 μM) of IgG1 monomer in 15 mM phosphate or MES solution with pH values ranging from 4.0 to 9.0.

Assessment of IgG1 stability in the sample solutions

To evaluate the stability of the IgG1 monomer in the sample solutions, the solutions were incubated at 60°C for 4 weeks or 80°C for 2 h. After incubation, the percentage of the residual IgG1 monomer and the percentage of soluble aggregates and degradates formed were evaluated by SEC–HPLC as follows: The unincubated sample solutions and the supernatants of incubated sample solutions (after centrifugation at 12,000 rpm for 5 min) were diluted with water to 1 mg/mL, applied to an HPLC

system (Waters) with a TSK–gel G4000SWXL column, and then eluted with 50 mM phosphate buffer, pH 7.0, containing 0.3 M NaCl.

The purity of the IgG1 monomer in the sample solutions was evaluated by SDS–PAGE with the following modifications: The unincubated sample solutions and uncentrifuged incubated sample solutions, without 2–mercaptoethanol, were diluted with buffer containing 10% SDS to obtain a final protein concentration of 100 μg/mL. The protein bands were stained with Coomassie brilliant blue. The stained gel was scanned using a photo scanner (Seiko Epson, Japan) to produce a high–resolution gray–scale image. The staining intensity of the monomer band in each sample was evaluated using "Scion Image" image analysis software (Scion Corporation, MD, USA) and the percentage of recovered monomer (unchanged monomer plus monomer released in the presence of SDS) in the sample solution was calculated from the ratio of the staining intensity in the incubated sample solution to the staining intensity in the corresponding unincubated sample solution.

Differential scanning calorimetry

DSC was carried out using a VP–DSC calorimeter (MicroCal). Each unincubated IgG1 monomer sample solution was diluted to 0.5 mg/mL by adding the same buffer solution, and then a DSC scan was performed at a rate of 0.5°C/min from 40°C to 105°C. Data were analyzed using Origin software (MicroCal).

Results

Aggregation of the IgG1 monomer during incubation

I evaluated the aggregation of the humanized IgG1 in phosphate or MES solutions with pH values ranging from 4.0 to 9.0 after incubation at 60°C for 4 weeks or at 80°C for 2 h. After incubation,

any insoluble aggregates that had formed were removed by centrifugation, and the solutions were analyzed by SEC–HPLC. As in Chapter I, I found both a higher molecular weight peak (soluble aggregates) and a lower molecular weight peak (degradates) after incubation at 60°C, but only a higher molecular weight peak after incubation at 80°C (Fig. II–1). The percentage of residual monomer and the percentage of soluble aggregates after incubation at 80°C are shown in Fig. II–2. The percentage of residual monomer and the percentages of soluble aggregates and degradates after incubation at 60°C are shown in Fig. II–3.

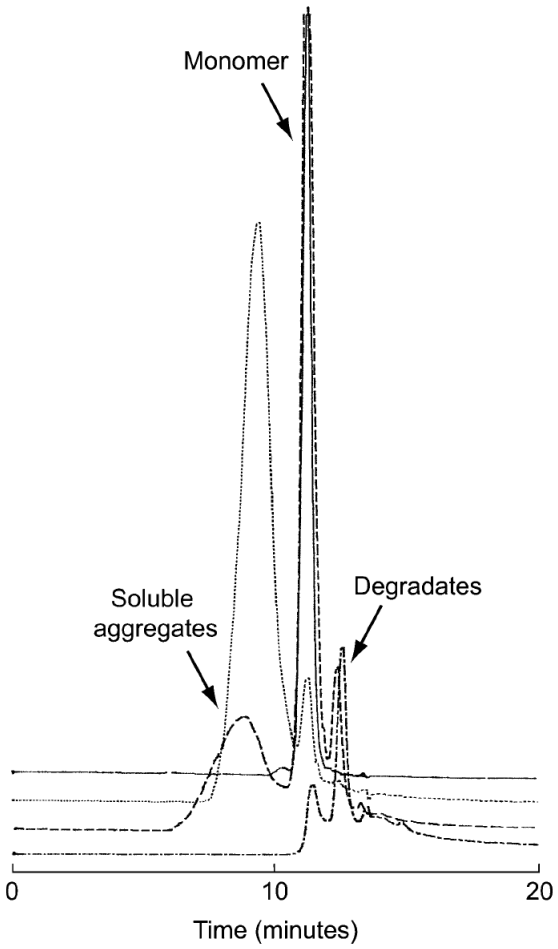

Fig. II–1 Typical size exclusion chromatograms of the humanized IgG1 in 15 mM MES (pH 4.0 or 6.5) before and after incubation. The solid line shows results found before incubation (pH 6.5); the other lines show results found after incubation under the following conditions: dotted line 80°C for 2 h (pH 6.5); broken line 60°C for 4 weeks (pH 6.5); dashed line 60°C for 4 weeks (pH 4.0)

After incubation at 80°C for 2 h, the percentage of residual monomer was relatively high at pH 4.0 and 5.0 but negligible at pH ≥ 7.0. In contrast, the pH profile of the percentage of soluble aggregates was bell–shaped, with a maximum between pH 6.0 and 7.0. The highest percentage of residual monomer was about 90% at pH 4.0 and 5.0 in MES.

After incubation at 60°C for 4 weeks, on the other hand, the pH profiles of the percentage of residual monomer and the percentage of soluble aggregates both showed maxima between pH 6.0 and 7.0 in both types of solution. Furthermore, insoluble aggregates were observed in both types of solution. This was consistent with the fact that the total percentages of monomer, soluble aggregates, and degradates did not add up to 100% at low or high pH levels.

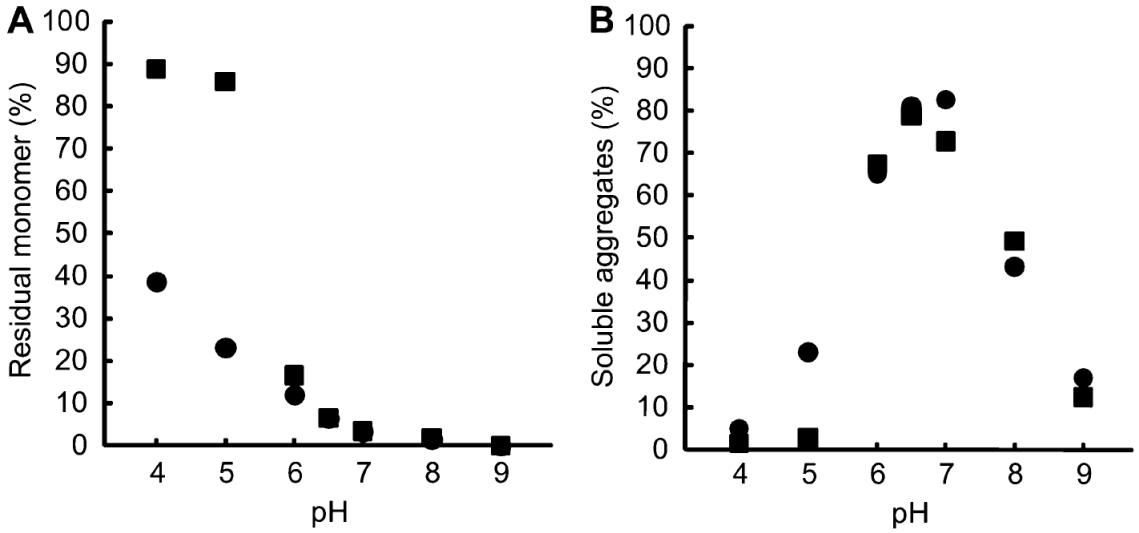

Fig. II–2 pH profiles of the percentages of residual monomer (A) and the soluble aggregate content (B) by SEC–HPLC after incubation of the humanized IgG1 in MES buffer (closed squares) or phosphate buffer (closed circles) at 80°C for 2 h.

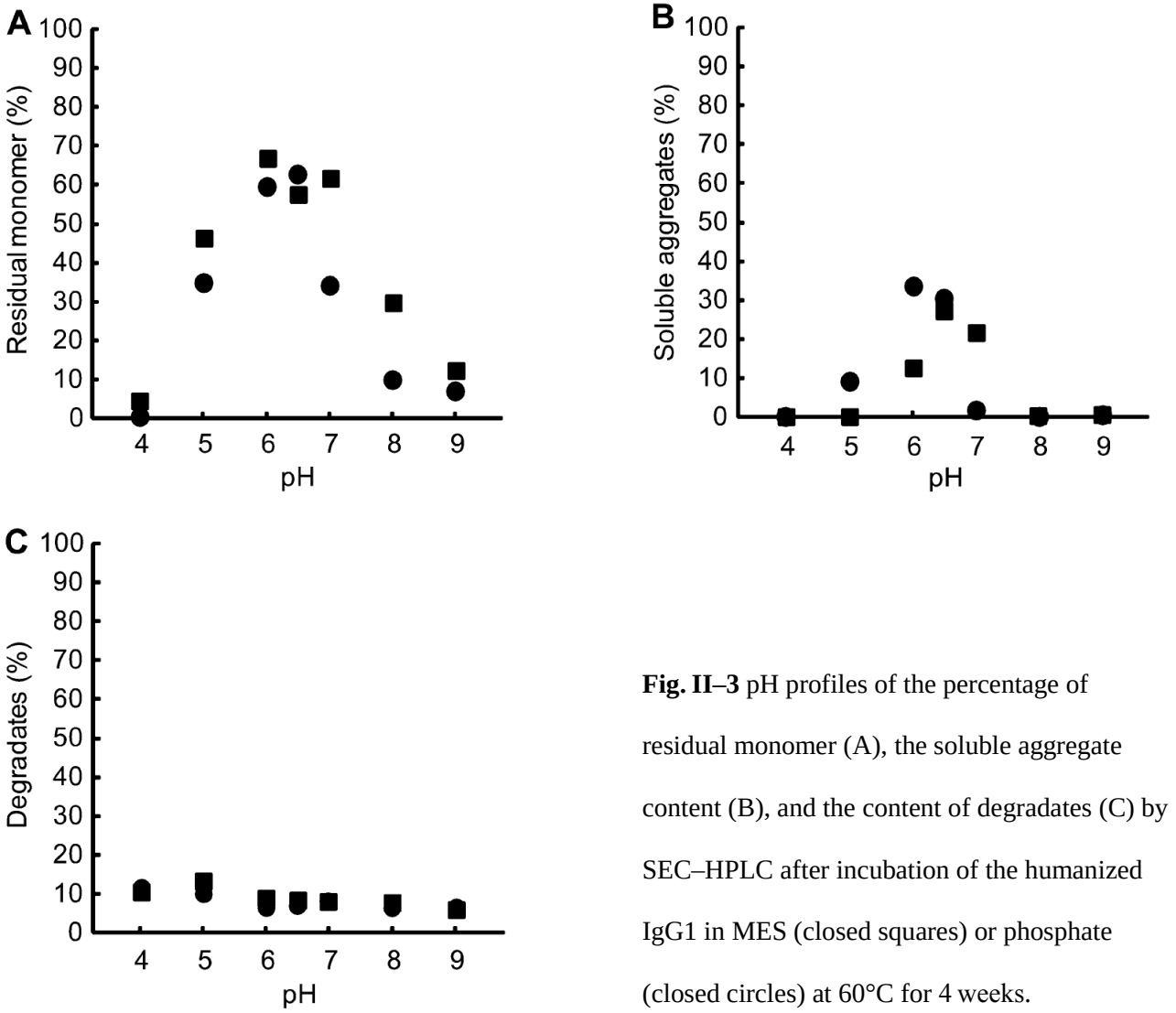

Fig. II–3 pH profiles of the percentage of residual monomer (A), the soluble aggregate content (B), and the content of degradates (C) by SEC–HPLC after incubation of the humanized IgG1 in MES (closed squares) or phosphate (closed circles) at 60°C for 4 weeks.

SDS–PAGE analysis of incubated IgG1 solutions

To evaluate whether the soluble aggregates form by covalent bonds and to find which peptide bond(s) in IgG1 molecule is cleaved, the incubated IgG1 solutions were analyzed by non–reducing SDS–PAGE. Typical electropherograms are shown in Fig. II–4. The IgG1 monomer band was detected at the same position as that of the molecular weight marker at about 200 kDa because of the presence of sugar chains.

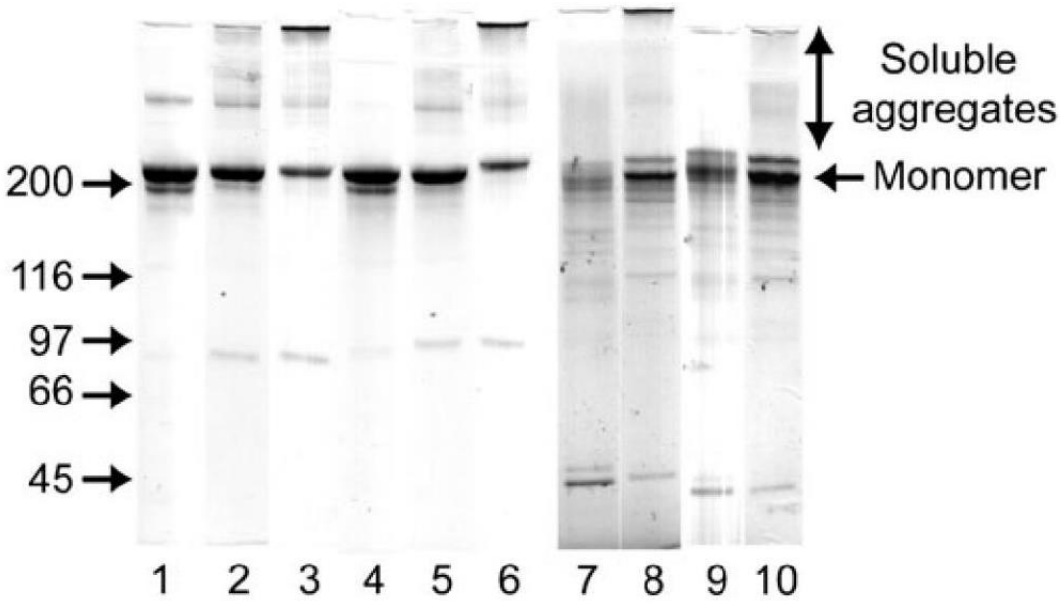

Fig. II–4 Non–reducing SDS–PAGE electropherograms after incubation of the humanized IgG1. Lanes 1–3 incubation at 80°C for 2 h in phosphate at pH 4.0, 6.0, and 8.0, respectively. Lanes 4–6 incubation at 80°C for 2 h in MES at pH 4.0, 6.0, and 8.0, respectively. Lanes 7 and 8 incubation at 60°C for 4 weeks in phosphate at pH 4.0 and 6.0. Lanes 9 and 10 incubation at 60°C for 4 weeks in MES at pH 4.0 and 6.0

After incubation at 80°C for 2 h, non–reducing SDS–PAGE revealed several bands at higher molecular weights than the monomer. Next, the percentage of recovered monomer was evaluated by densitometry. The percentage of recovered monomer decreased with increasing pH (Fig. II–5). At pH 8.0 and 9.0, the overall band intensity decreased because of the formation of insoluble aggregates that remained insoluble even in the presence of SDS. From the viewpoint of difference in solution types, in contrast to the SEC–HPLC, the percentages of recovered monomer contents in the MES and phosphate sample solutions were comparable. From these results, I found that the aggregates present after incubation at 80°C for 2 h in MES or phosphate had mainly formed by non–covalent interactions rather than covalent bonds and that aggregates formed under acidic conditions were soluble in the presence of SDS. I also found that MES retarded aggregation during incubation at 80°C in the condition at pH 4.0 and 5.0. However, a single band (Unknown–1) was

observed on the high molecular weight side of the H chain at pH 8.0 and 9.0 in reducing SDS–PAGE, suggesting the formation of non–disulfide covalent bonds.

After incubation at 60°C for 4 weeks, non–reducing SDS–PAGE showed a broad band on the high molecular weight side of the monomer. Densitometry revealed maximum monomer content in the pH range of 5.0 to 6.0 in both types of buffer (Fig. II–5). At higher pH levels, most of the bands disappeared because of the formation of insoluble aggregates that remained insoluble even in the presence of SDS, as with incubation at 80°C for 2 h. At pH 4.0 and 5.0, on the other hand, the percentage of recovered monomer content in both types of buffer was higher than that detected by SEC–HPLC, indicating that the soluble and insoluble aggregates present after incubation at 60°C for 4 weeks at pH 4.0 and 5.0 had mostly formed by non–covalent interactions that could be broken by the addition of SDS, releasing monomer.

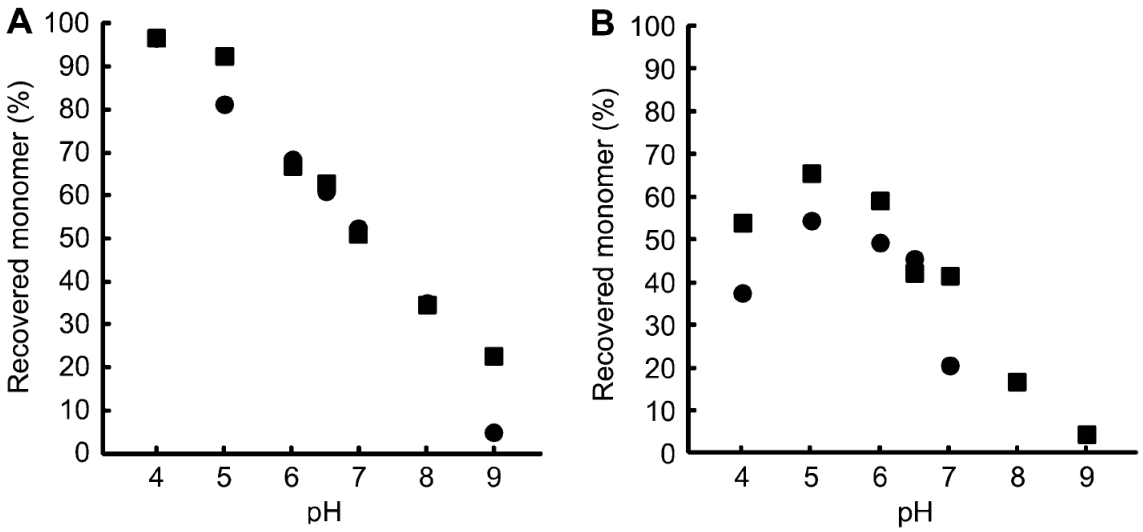

Fig. II–5 The pH profiles of the percentage of recovered monomer by densitometry of scanned non–reducing SDS–PAGE electropherograms after incubation of the humanized IgG1 in MES (closed squares) or phosphate (closed circles) at 80°C for 2 h (A) or at 60°C for 4 weeks (B).

Unfolding temperatures of the IgG1 molecule

I evaluated the influence of pH on the unfolding temperature of the IgG1 in phosphate or MES by DSC. I already revealed in Chapter I that the unfolding of the IgG1 was able to be divided into three steps. The first two steps involve unfolding of the Fc domain; the third step involves unfolding of the Fab domain. From the results, the unfolding temperatures in the first and second steps were lower at pH 4.0 and 5.0 in both types of solution (Fig. II–6). In particular, the unfolding temperature in the first step was markedly lower at those pH levels: 60–63°C and 63–65°C in phosphate and MES, respectively. In addition, an exothermic signal appeared during the third unfolding step at higher pH levels, suggesting that aggregation of the unfolded intermediate of IgG1 occurs at that point. The exothermic signal was found at pH $\geq$ 6.0 in phosphate, but only at pH 8.0 and 9.0 in MES.

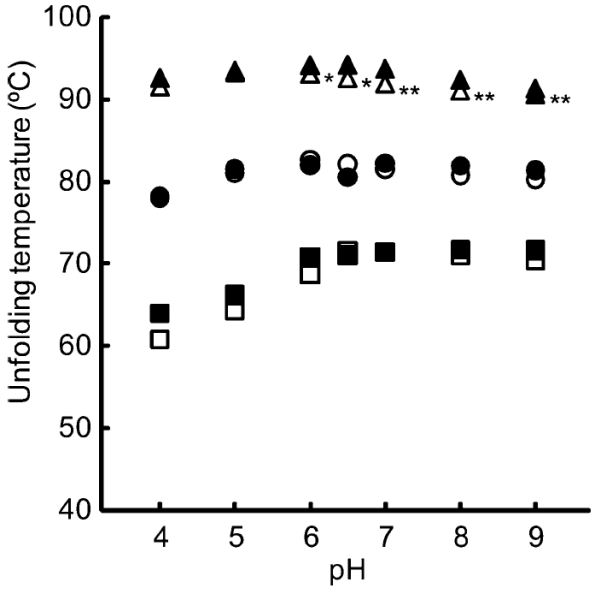

Fig. II–6 The pH profile of the unfolding temperature of each unfolding step of the humanized IgG1 molecule. Closed symbols indicate MES (closed squares, first step; closed circles, second step; closed triangles, third step). Open symbols indicate phosphate (open squares, first step; open circles, second step; open triangles, third step). Asterisks (* or **) indicate that an exothermic signal was observed during the third unfolding step, either in phosphate only (*) or in both types of solutions (**). These exothermic signals suggest aggregation of the humanized IgG1

Discussion

Effect of the conformational stability of the C_H2 domain on the aggregation of the humanized IgG

Acidic conditions are crucial for the purification of humanized IgGs in Protein A affinity columns and for virus inactivation. To examine the aggregation and peptide bond cleavage of the humanized IgG1 investigated in this chapter under both acidic and weakly alkaline conditions, I used SEC–HPLC and SDS–PAGE to evaluate the percentage of residual monomer in solutions that had been incubated in phosphate or MES at pH levels ranging from 4.0 to 9.0.

After incubation at 80°C for 2 h, non–reducing SDS–PAGE showed gradual decrease in the percentage of residual monomer with an increase in incubation pH. In Chapter I, I reported that aggregation of the IgG1 was initiated by denaturation of the Fc region. Moreover, a recent report indicated that the IgG1 C_H2 domain had the lowest stability among human immunoglobulin domains [21]. Therefore, since the C_H2 domain was shown to unfold at temperatures below 80°C in the pH range of 4.0 to 9.0 (the first unfolding step in Fig. II–8), IgG1 incubated at 80°C for 2 h should form an unfolded intermediate in which the C_H2 region is denatured. Moreover, since the isoelectric point of IgG1 is estimated to be around 9, severe aggregation of the IgG1 monomer should tend to occur with increasing storage pH up to 9. This suggests that the pH dependency of the monomer content by non–reducing SDS–PAGE after incubation at 80°C for 2 h (Fig. II–4) is caused by severe IgG1 aggregates that remain insoluble even in the presence of SDS. I therefore showed that unfolded IgG1 intermediate was deeply involved in aggregate formation in this chapter. Although such pH–dependent aggregation is found in many proteins, including IgG, different patterns are seen in different proteins. For example, when LA298 (a humanized IgG1 antibody of the same subclass as the IgG investigated in this chapter) was stored at 25°C, aggregation occurred only in phosphate buffer at pH 7.0 or 8.0 and was not detectable in citrate buffer at pH 4.0 to 7.0,

although the low IgG1 concentration (0.5 mg/mL) may have inhibited aggregation [24]. On the other hand, the pH profile of the aggregation rate of a 100 mg/mL IgG2 solution was inverted by changing the storage temperature. That is, the pH profile of the aggregation rate was pH 5.5 < pH 5.2 < pH 5.0 on storage at 37°C, but was pH 5.0 < pH 5.2 < pH 5.5 on storage at 29°C [25]. Moreover, IgG4 aggregation rates were affected by exposure to the acidic condition of pH 2.7, because of change in the higher–order structure of the IgG4 molecule [11].

Inhibitory effect of MES buffer on aggregation of humanized IgG1 over a wide pH range

In Chapter I, I reported the inhibitory effect of MES solution on the aggregation at pH 5.5 and 6.5 of the IgG1. In this chapter, comparison between the results in phosphate and MES solutions showed that MES buffer gave high stability regardless of pH and incubation conditions. In particular, the percentage of residual monomer after incubation at 80°C in the range of pH 4.0 to 5.0 and after incubation at 60°C in the range of pH 7.0 to 8.0 differed markedly depending on the solution types. These differences suggested that MES inhibited aggregation of the IgG1 over a wide pH range. As described in the previous studies including that in Chapter I, IgG1 aggregation was initiated by denaturation of the Fc region [21]. Based on the thermal stability of the IgG1 at various solution pH levels (Fig. II–8), unfolded intermediates of the IgG1 with a partially or fully denatured Fc region will form under the storage conditions where I used (incubation at 80°C for 2 h or incubation at 60°C for 4 weeks). Under these conditions, interactions between MES and unfolded intermediates may retard aggregation of the IgG1. Recently, nuclear magnetic resonance (NMR) analysis has revealed that an interaction between human liver fatty acid uniting protein and the MES molecule occurs in the order of microseconds to milliseconds [26]. The MES molecule consists of a hydrophilic group and a hydrophobic group. Additional experiments using techniques such as NMR

would be needed to elucidate the interaction between the MES molecule and polypeptide chains. For the present, I have demonstrated in this chapter that MES inhibits aggregation of the IgG1 in the pH ranges of 4.0 to 5.0 and 7.0 to 8.0.

CHAPTER III

Effect of the Conformational Stability of the C_H2 Domain on the Peptide Cleavage of a Humanized IgG

Abstract

In Chapter II, I revealed that the pH dependency of humanized IgG aggregation could be accounted for by (1) the decrease in unfolding temperature of the first step due to the increased instability of the C_H2 domain at lower pH and (2) the increase in the aggregation propensity of heat–denatured intermediates at higher pH. In this chapter, I evaluated the deterioration of humanized IgG using reduced SDS–PAGE analyses of sample solutions incubated at various pH levels. I selected MES and phosphate as the buffer agents, and the samples were incubated at 60°C and 80°C. From the results, a decrease in residual H chain and the formation of unknown molecular species were observed after the long incubation at 60°C, and these tendencies were predominant under acidic conditions. Using the Edman degradation technique, I confirmed that these phenomena were due to cleavage of the Asp272–Pro273 peptide bond in the C_H2 domain. Furthermore, a comparison of the cleavage rates of the IgG1 monomer and a peptide containing the same Asp–Pro sequence revealed that the conformational stability of the C_H2 domain retarded cleavage of the Asp272–Pro273 peptide bond at 60°C and pH 4.0. From these results, I found that the conformational stability of the C_H2 domain was closely related to peptide cleavage of the humanized IgG1 under acidic conditions.

Introduction

A number of biologically important and functional proteins including immunoglobulin have marginal stability in solution, and are easily degraded under environmental conditions with different

types of applied stress. In general, protein instabilities are separated into two classes: physical instability and chemical instability. Physical instability occurs with changes in the higher–order structure and may induce protein aggregation. In Chapter I and II, I have discussed the effects of solution conditions such as buffer species or pH on protein aggregation using humanized immunoglobulin. Chemical instabilities involve non–enzymatic processes that make or break covalent bonds, resulting in new chemical entities. Non–enzymatic reactions sometimes take place at the side chains of amino acids, and the biological activity and immunogenicity of proteins may be influenced by these undesirable chemical reactions [27, 28]. For example, the effects of iso–Asp formation have been examined in numerous cases, including aggregation and loss of activity [29, 30]. Moreover, interaction between the Fc region of IgG and neonatal Fc receptor (FcRn) plays a critical role in regulating IgG homeostasis. In fact, it has been reported that some mutations of IgG improve the pharmacodynamic properties [31], and that report implies that it is chemical modifications of IgG that may alter such properties. Therefore, researchers should focus not only on the mechanisms of aggregation, but also on the chemical reactions of humanized IgGs.

Several types of chemical modification reaction are responsible for chemical instability. Most frequently described reactions are deamidation, hydrolysis, oxidation, reduction, β–elimination, and racemization. The nature and mechanisms of these reactions are extensively reviewed in the literature [32]. Deamidation of asparagine and glutamine have been the most extensively studied among the chemical reactions in proteins and peptides [33–35]. In addition to that, hydrolysis of amide bonds also has an impact on the stability of proteins and peptides [36].

In assessing the purity and integrity of biopharmaceuticals such as humanized IgG, fragmentation is a critical quality attribute that needs to be monitored [37]. Fragmentation can occur during protein production in the cell culture, and is modulated by the purification process and accrues during storage or circulation in the blood. Although the protein backbone of IgG is extremely stable under physiological conditions, certain sites may become prone to fragmentation

as a function of the amino acid sequence, flexibility of the local structure, solvent conditions (pH and temperature), and the presence of metals or radicals. There are several studies on peptide bond cleavage of proteins, and Asp–Pro is the sequence that is hydrolyzed and cleaved most frequently under acidic conditions. For example, a recombinant MUC2 C terminus expressed in Chinese hamster ovary (CHO)–K1 cells was partly cleaved at the Asp–Pro bond during purification, and such cleavage occurred in a time–dependent manner at a pH of below 6.0 [38].

In this chapter, I evaluated the effect of formulation pH on deterioration of a humanized IgG under two different buffer conditions using quantitative SDS–PAGE with densitometry. The buffers used in this chapter are phosphate and MES, which are same as those used in Chapter II. I found that the content of H chain after storage at 60°C was decreased under acidic conditions resulting that the decrease was caused by the cleavage of Asp–Pro bonds in the H chain. Furthermore, I compared the rate of cleavage of Asp–Pro bonds between whole IgG and a peptide that included the sequences around the cleavage site in order to show the effect of the higher–order protein structure on chemical modification.

Materials and Methods

Materials and reagents

The IgG molecule investigated in this chapter was the same monoclonal antibody used in Chapter I. The TSK–gel G4000SWXL column (7.8 × 300 mm) used was purchased from Tosoh (Tokyo, Japan).

Preparation of the IgG1 monomer sample solutions

I prepared the same sample solutions for evaluation as Chapter II from an IgG1 stock solution.

Assessment of IgG1 stability in the sample solutions

To evaluate the stability of the IgG1 monomer in the sample solutions, the solutions were incubated at 60°C for 4 weeks or 80°C for 2 h. After incubation, the purity of the IgG1 monomer in the sample solutions was evaluated by SDS–PAGE using the method of Laemmli [12] with the following modifications: The unincubated sample solutions and uncentrifuged incubated sample solutions, with 2–mercaptoethanol, were diluted with buffer containing 10% SDS to obtain a final protein concentration of 100 µg/mL. The protein bands were stained with Coomassie brilliant blue. The stained gel was scanned using a photo scanner (Seiko Epson, Japan) to produce a high–resolution gray–scale image. The staining intensity of bands that corresponded to H and L chains in each sample was evaluated using "Scion Image" image analysis software (Scion Corporation, MD, USA) and the percentage of residual H and L chains in the sample solution was calculated from the ratio of the staining intensity in the incubated sample solution to the staining intensity in the corresponding unincubated sample solution.

N–terminal amino acid sequence analysis

I analyzed the N–terminal amino acid sequences of unknown bands in the reducing SDS–PAGE electropherograms by the Edman degradation method using Protein Sequencer 473A (Applied Biosystems, CA, USA), after transferring the bands to a polyvinylidene fluoride (PVDF) membrane.

Evaluation of Asp–Pro cleavage in the IgG and a corresponding peptide

A 10 mg/mL IgG1 solution in 15 mM acetate (pH 4.0) was incubated for 1, 2, and 4 weeks. The intact H chain content was determined by densitometry of scanned SDS–PAGE electropherograms as described above, and the percentage of residual intact H chain was calculated.

A 15–residue peptide with the sequence VDVSHEDPEVKFNWY was prepared by Fmoc solid–phase peptide synthesis. This peptide was dissolved in 15 mM acetate buffer to give a concentration of 66.7 μM, which is of the same molar concentration as the 10 mg/mL IgG1 solution. The percentage of the residual peptide after incubation for 6, 12, 18, 24, and 36 h at 60°C was found by reverse–phase high–performance liquid chromatography (RP–HPLC) using an HPLC system (Hitachi, Japan) with a TSK–gel ODS–120T (250 mm × 4.6 mm–i.d.) column (Tosoh, Japan). The compositions of mobile phases A and B were (A) 1% acetonitrile and 0.05% hydrochloric acid and (B) 60% acetonitrile and 0.05% hydrochloric acid. Peaks were found by detection at 350 nm. A sample solution containing 3.3 nmol of peptide was injected, and the percentage of residual intact peptide was found from the ratio of the intact peptide peak areas in incubated and unincubated samples.

Results

SDS–PAGE analysis of incubated IgG1 solutions

In reducing SDS–PAGE, there were three additional bands on the high molecular weight side of the H chain band (Unknown–1) and on each side of the L chain band (Unknown–2 and Unknown–3) after the incubation at 60°C for 4 weeks in the condition at pH 4.0 (Fig. III–1). Moreover, the intensity of H chain band after the incubation at 60°C for 4 weeks was markedly decreased at pH 4.0. However, marked change of electrophoregram was not observed after the incubation at 80°C for 2h. The percentages of residual H and L chains in solutions incubated at pH 4.0, 5.0, 6.0, and 6.5 for 4 weeks at 60°C are shown in Fig. III–2. The percentage of residual H chain decreased with decreasing pH in both types of solution, whereas the percentage of residual L chain showed quantitative recovery at pH 4.0 and gradually decreased with increasing pH. These results suggested

that Unknown–2 and Unknown–3 were derived from the H chain. On the other hand, it was considered that Unknown–1 was attributed to the formation of non–disulfide covalent bonds.

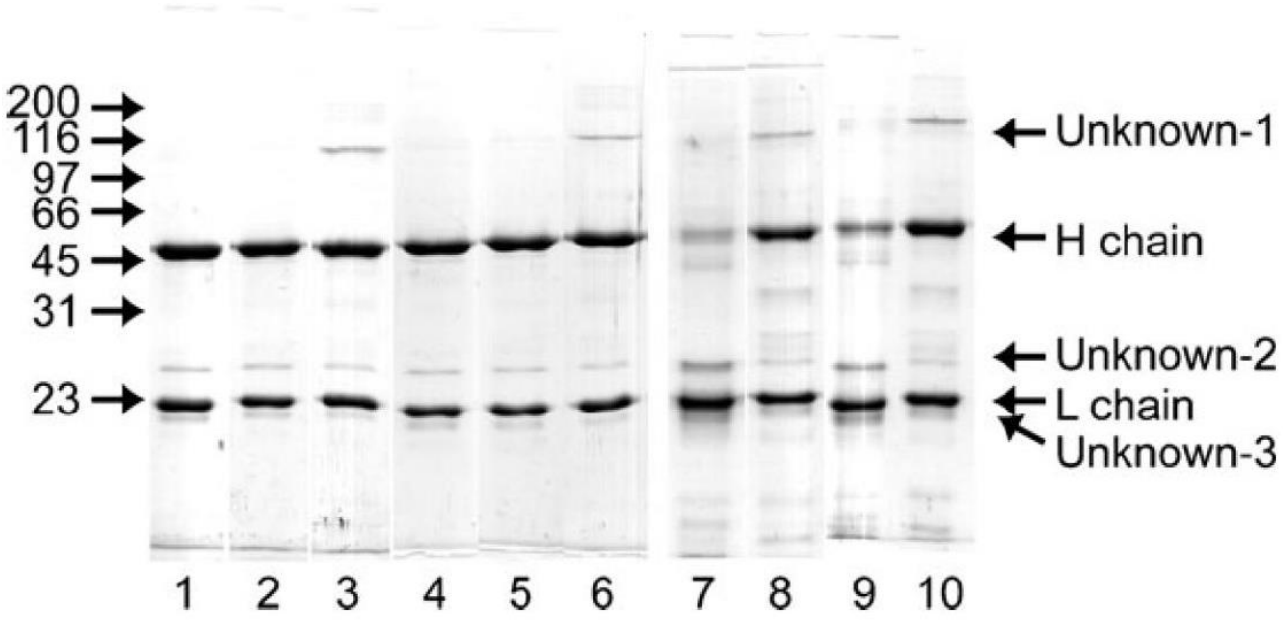

Fig. III–1 Reducing SDS–PAGE electropherograms after incubation of the humanized IgG1. Lanes 1–3 incubation at 80°C for 2 h in phosphate at pH 4.0, 6.0, and 8.0, respectively. Lanes 4–6 incubation at 80°C for 2 h in MES at pH 4.0, 6.0 , respectively, and 8.0. Lanes 7 and 8 incubation at 60°C for 4 weeks in phosphate at pH 4.0 and 6.0. Lanes 9 and 10 incubation at 60°C for 4 weeks in MES at pH 4.0 and 6.0

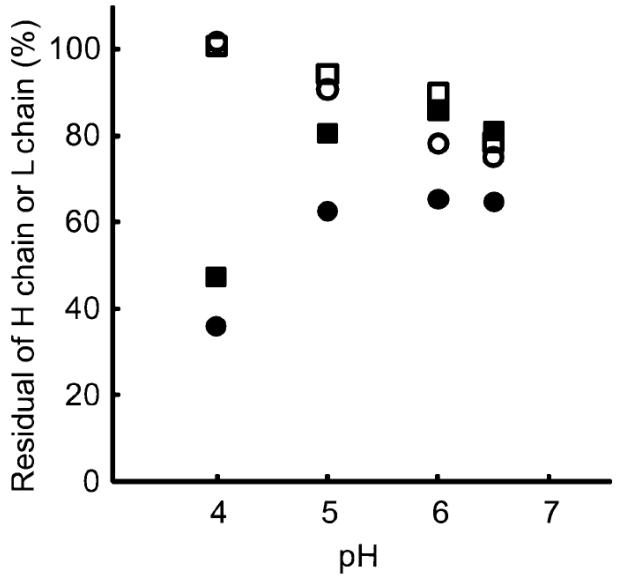

Fig. III–2 The pH profiles of the percentages of residual H and L chains by densitometry of scanned reducing SDS–PAGE electropherograms after incubation of the humanized IgG1 at 60°C for 4 weeks. Squares indicate MES (closed squares, H chain; open squares, L chain). Circles indicate phosphate (closed circles, H chain; open circles, L chain)

Cleavage site during incubation at 60°C for 4 weeks in the condition at pH 4.0

To identify Unknown–2 and Unknown–3, I analyzed their peptide sequences using a peptide sequencer. The N–terminal sequence of the peptide in Unknown–2 was Pro–Glu–Val–Lys–Phe, but that of the peptide in Unknown–3 could not be determined. Based on the amino acid sequence of the IgG1 H chain, I identified the cleavage site as the Asp272–Pro273 peptide bond in the IgG1 C_H2 domain. The N–terminal residue of the IgG1 H chain was glutamine, which can readily cyclize as pyroglutamic acid. Pyroglutamic acid cannot be sequenced by the method I used (Edman degradation). Therefore, failure to determine the N–terminal sequence in Unknown–3 would be due to the formation of N–terminal pyroglutamic acid in Unknown–3 during incubation at 60°C for 4 weeks in the condition at pH 4.0.

Kinetics of Asp–Pro cleavage during incubation at 60°C in the condition at pH 4.0

To examine the effect of the conformational stability of the IgG1 C_H2 domain on cleavage of the Asp–Pro peptide bond, I incubated IgG1 H chain and 15–residue peptide (VDVSHEDPEVKFNWY,

corresponding to Val266–Tyr280 of the IgG1 H chain) at 60°C in the condition at pH 4.0 in 15 mM acetate (in which the 15–residue peptide has higher solubility than in MES or phosphate). After incubation, I evaluated the percentage of residual IgG1 H chain by reducing SDS–PAGE, and the percentage of residual intact 15–residue peptide by RP–HPLC (Fig. III–3). The percentage of the residual 15–residue peptide was 50% after only half a day, whereas the percentage of residual IgG1 H chain was still above 75% after a week. In the case that this cleavage can be assumed as the first–order reaction, the reaction rate constant of Asp–Pro cleavage is calculated to be $-4.1 \times 10^{-2}\ h^{-1}$ for the 15–residue peptide and $-1.6 \times 10^{-3}\ h^{-1}$ for the IgG1 H chain. Therefore, the cleavage rate of the IgG H chain is about 25 times as slow as that of the 15–residue peptide.

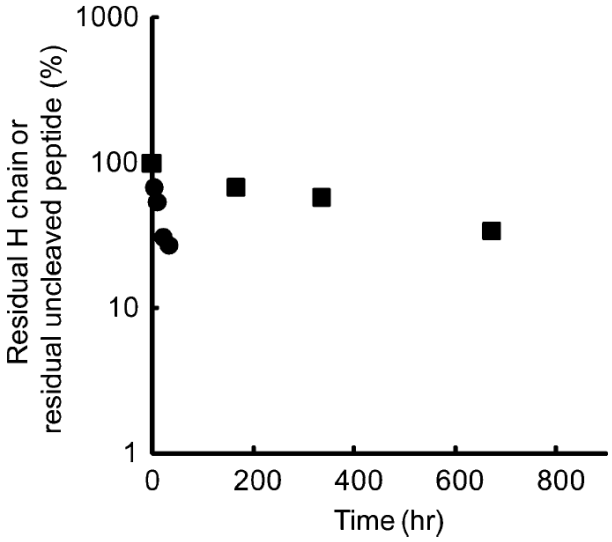

Fig. III–3 Time courses of the percentage of residual H chain (closed squares) in an IgG1 solution and the percentage of residual uncleaved peptide (closed circles) in a solution of a peptide corresponding to the IgG1 H chain Asp–Pro sequence, during incubation at 60°C. Both solutions were prepared using 15 mM acetate (pH 4.0)

Discussion

Effect of the conformational stability of the C_H2 domain on peptide cleavage of the humanized IgG1

Acid treatment is an indispensable process in the purification of biopharmaceuticals such as antibody drugs. To examine the chemical modification and peptide bond cleavage of the humanized IgG1 investigated in this chapter under both acidic and weakly alkaline conditions, I used SDS–PAGE to evaluate the percentage of the residual H and L chains in solutions that had been incubated in phosphate or MES buffer at pH levels ranging from 4.0 to 9.0. After incubation at 60°C for 4 weeks, the percentage of residual H chain decreased with decreasing pH in both types of buffer, whereas the percentage of residual L chain showed a quantitative recovery at pH 4.0 and gradually decreased with increasing pH. These results suggested that Unknown–2 and Unknown–3 were derived from the H chain. That is, this phenomenon may be the result of cleavage of the Asp272–Pro273 peptide bond in the IgG1 H chain under acidic conditions. This assumption is reasonable because the cleavage of Asp–Pro under acidic conditions is well–known [39], in which the only Asp–Pro peptide bond in the IgG is the Asp272–Pro273 peptide bond in the H chain. In Chapter II, it was shown that the pH–dependency of recovered monomer in the presence of SDS was different between incubation at 60°C for 4 weeks and that at 80°C for 2 h. After incubation at 80°C for 2 h, the percentage of recovered monomer was directly proportionate to pH levels and was highest under the most acidic condition (pH 4.0). On the other hand, after incubation at 60°C for 4 weeks, the relationship between the percentage of recovered monomer and pH levels showed a bell–shaped curve, and the percentage of recovered monomer at pH 4.0 was lower than that at neutral pH. Therefore, the cleavage of Asp–Pro was shown as one of the most important types of chemical modification, resulting in the reduced stability of humanized IgG1 under acidic conditions.

The difference between the monomer content found by SEC–HPLC and that by non–reducing SDS–PAGE at pH 4.0 could not be explained by the degradate contents found by SEC–HPLC at pH 4.0 alone. This fact implies that IgG1 nicked at the Asp–Pro bond is present among the insoluble aggregates formed after incubation at 60°C for 4 weeks in the condition at pH 4.0. Interestingly, as described in Chapter II, the unfolding temperatures of the first transition in the IgG1 were 60–63°C in the condition at pH 4.0 and 63–65°C in the condition at pH 5.0. In fact, the first transition was suggested to be the result of denaturation of the IgG1 C_H2 domain [21, 40], and the Asp272–Pro273 peptide bond, which is located in the C_H2 domain, was hydrolyzed at pH 4.0. From these results in this chapter, I found that there was a similar tendency between the hydrolysis of the Asp–Pro peptide bond and the conformational stability of the IgG1 C_H2 domain. Therefore, it may be considered that the Asp272–Pro273 peptide bond cleavage during long incubation at 60°C in the condition at pH 4.0 and 5.0 would occur in an unfolded intermediate in which the C_H2 domain is denatured. To clearly show the contribution of structural stability to Asp–Pro peptide bond cleavage, I compared the Asp–Pro peptide bond cleavage rate in the whole humanized IgG1 with that in the peptide corresponding to Val266–Tyr280 of the IgG1 H chain. The cleavage rate of the IgG H chain was found to be one–twenty–fifth the cleavage rate of the 15–residue peptide. Therefore, the conformational stability of the IgG1 molecule is expected to retard non–enzymatic cleavage of the Asp272–Pro273 peptide bond in the IgG1 C_H2 domain.

There were some reports suggesting the contribution of structural stability to the chemical stability of proteins. For example, the more stabilized hen egg white lysozyme was reduced in the deterioration rate on incubation at pH 4 and 100°C [41], and chemical reactions such as deamidation and racemization in hen egg white lysozyme were depressed by sucrose and trehalose due to tertiary structures including α–helical structures being induced in the polypeptide chain [42]. Evaluation of the chemical stability of recombinant human lymphotoxin (rhLT) also revealed that the stability against Asn deamidation can be accounted for by the structural stability rather than the

primary sequences [43]. In fact, the deamidation rates of two Asn sites (Asn19 and Asn40–Asn41) in rhLT were much slower than those in model peptides, but these rates were markedly accelerated by denaturation. In particular, the deamidation rate of Asn19 after denaturation was almost the same as that of the model peptide. From these references, the finding in this chapter that the stability of the Asp–Pro sequence was much higher in human IgG than in the model peptide was a result of the structural stability of human IgG. Therefore, the lower stability of Asp–Pro sequence at pH 4.0 was able to be accounted for by the lower stability of the C_H2 domain at this pH.

Significance of this findings for the development of humanized IgGs as pharmaceuticals

As described in the introduction to Chapter II, elution of IgGs from Protein A affinity columns during purification of therapeutic antibodies is carried out under acidic conditions at pH 4.0 to 5.0. Since the Asp–Pro sequence in the H chain of the C_H2 domain is conserved in humanized IgGs, the findings in this chapter imply that it is necessary to pay attention to Asp–Pro cleavage during the treatment of therapeutic antibodies using Protein A columns. In general, it is considered that humanized IgGs induce very little immune response in the human body. However, therapeutic antibodies are sometimes used in patients who have their own individual human leukocyte antigen systems. As a result, the cleavage of the peptide bond at Asp272–Pro273 in humanized IgGs could induce autoantibodies because peptide fragmentation of self–proteins has been reported to induce cryptic determinants that trigger the production of autoantibodies [44]. Therefore, since even small amounts of foreign proteins or peptides generally cause immune reactions, I should pay close attention to impurities in humanized antibodies resulting from cleavage of the H chain Asp–Pro peptide bond.

CHAPTER IV

Method of Detecting Asparagine Deamidation and Aspartate Isomerization for Evaluation of Deterioration in Humanized IgG

Abstract

A method was established for evaluating Asn deamidation and Asp isomerization/racemization. To detect the subtle changes in mass that accompany these chemical modifications, I used a combination of enzyme digestion by endoproteinase Asp–N, which selectively cleaves the N–terminus of L–α–Asp, and MALDI/TOF–mass spectrometry. L–Asn residue is deamidated into L–Asp, which is recognized and cleaved by endoproteinase Asp–N; on the other hand, L–Asp residue is isomerized into β–Asp (iso–Asp) and D–Asp which is not recognized by endoproteinase Asp–N. That is, the molecular weight and number of digestion fragments will change in MALDI/TOF–mass spectrometry analysis because the number of sites recognized by endoproteinase Asp–N is influenced by such chemical changes. To demonstrate the advantages of this method, I applied it to identify deamidated sites in mutant lysozymes in which the Asn residue is mutated to Asp. Moreover, I also identified the deamidation or isomerization sites of the lysozyme samples after incubating them under acidic or basic conditions. Therefore, this detection method would be applicable for detecting Asn deamidation and Asp isomerization which are critical mechanisms of deterioration of biopharmaceuticals including humanized IgG.

Introduction

Amino acid side chains or peptide backbones of proteins are susceptible to various non–enzymatic chemical reactions under physiological conditions, including deamidation, racemization, isomerization, β–elimination, exchange of disulfide bonds, and oxidation. In particular, deamidation of Asn or Gln [41, 45–51], and isomerization/racemization of Asp [41, 50–55] were frequently reported. These reactions were generally accelerated at higher temperatures, and they have different pH–dependencies. If such a chemical reaction occurs at the active center of an enzyme, the enzyme will be inactivated very easily. On the other hand, when various chemical modifications accumulate, a protein lost its native conformation and thereby its function [45, 46].

Deamidation involved hydrolysis at an amide bond of Asn and Gln, and it occurred under physiological conditions [34]. Moreover, deamidation was promoted under basic conditions and occurred more easily at Asn than at Gln. In particular, significant reaction rates have been observed under neutral pH conditions, when the Asn residue is followed by Gly in the sequence of amino acids, because Asn has a marked tendency to form the succinimide intermediate in such conditions [33, 34, 56]. Deamidation is the most probable reaction by which proteins are degraded during cell culture, purification, and preservation. Deamidation is known to lead to heterogeneity in terms of quality, and it also is known to decrease the activity of an enzyme. For example, serine hydroxymethyltransferase purified from rabbit liver cytosol with two deamidated Asn residues (Asn5 and Asn220) had lower catalytic activity than the recombinant enzyme in the non–deamidated form [47]. The heterogeneity of purified murine monoclonal antibody MMA383 was mainly due to deamidation at Asn141 in its heavy chain and at Asn161 in its light chain [48]. Asn107 in aged PrP was converted to Asp by a spontaneous pathway involving deamidation, resulting in an increase in the β–sheet content and a tendency to form aggregates [49]. Such covalent variants of PrP^{C} may generate PrP^{Sc}–like species, which initiate fatal prion diseases, such as Creutzfeldt–Jakob disease.

The Asp–X peptide bond is easily isomerized or racemized via the succinimide intermediate, and L–Asp becomes β–Asp (iso–Asp) and D–Asp. The succinimide intermediate hydrolytically divided into a β–Asp/α–Asp mixture at an approximate ratio of 3:1 in the hydrolysis of the ethyl ester of *N*–benzoyl–β–aspartylglycine *n*–hexylamide [57]. The formation of succinimide at Asp occurs most easily when Asp is followed by Gly. The optimum pH for its formation is pH 4–5. Many examples of the protein isomerization of Asp have been reported in basic fibroblast growth factor and insulin, where the main deterioration products are the result of isomerization of Asp residues [52, 53]. Isomerization and inversion have been observed in the course of human aging. For example, the D/L–ratio of Asp residues (Asp58, Asp151) in αA–crystallin from human eye lenses increased with age [54, 55]. In the case of deamidation, Asp derived from Asn was often racemized, as was observed in tissue plasminogen activator [50]. Site–specific deamidation and isoaspartate formation in tau proteins in the brain caused aggregation and resulted in paired helical filament formation *in vivo* [51].

Mass spectrometry is a powerful method to identify chemical modifications in proteins, because such modifications cause changes in the mass of protein. Mass spectrometry is often combined with peptide mapping on reversed–phase HPLC after digestion by trypsin or other enzymes, because the combination of these methods is not only highly sensitive but also enables identification of the modified position. For example, by the combination of these methods using MALDI/TOF–mass spectrometry, the oxidation of four methionine residues was identified in H_2O_2–treated nucleoside diphosphate kinase, because a 16 Da increase in the mass was observed in the oxidized peptide [58]. Moreover, methionine residues that are susceptible to oxidation in recombinant human 1–antitrypsin were identified and quantified using a combination of the above methods [59]. When mass spectrometry is applied to identify deamidation, isomerization, and racemization, the subtle differences in the mass of the protein can pose a problem. Namely, the mass of protein/peptide changes by only 1 Da in the case of deamidation, and does not change in the case of either

isomerization or racemization. Indeed, to detect deamidation, isomerization, and racemization, the separation of peptides on reverse–phase HPLC was required in the case of lysozymes and cAMP–dependent protein kinase [60, 61]. Edman sequencing is useful for identifying isomerization and racemization, because these reactions stop at the isopeptide bond. Recent improvements in the accuracy and sensitivity of mass spectrometry have allowed the identification of deamidated Asn in proteins by detecting a subtle change in the mass of proteins of only 1 Da [48, 49]. However, achieving total accuracy by mass spectrometry would require extra experimental techniques. As I described in Chapter III, Asp272‐Pro273 in C_H2 domain of IgG was a factor of deterioration of IgG. In the future, it is expected that more human antibodies are applied as pharmaceuticals. The specificity of IgG was derived from the specific amino acid sequence of CDR region in Fab. As a result, numerous sequences can occur at the CDR regions and some of those sequences will include the site which is prone to be deamidated or racemized. Therefore, it would be important that the identification of deamidation or racemization site in IgG molecule for developing functional IgG as pharmaceuticals.

In this chapter, I developed a convenient method for detecting deamidation of Asn and isomerization/racemization of Asp in a protein, using a combination of mass spectrometry and peptide mapping with endoproteinase Asp–N (Fig. IV–1). Endoproteinase Asp–N is a specific protease that cleaves the N–terminus amide bond of L–α–Asp [62]. When Asn is deamidated to Asp in proteins or peptides, the product will be hydrolyzed by endoproteinase Asp–N and will increase the number of signals on mass spectrometry. On the other hand, when L–α–Asp in proteins or peptides is isomerized to L–β–Asp or racemized to D–Asp, the product is not hydrolyzed by endoproteinase Asp–N, and the number of signals on mass spectrometry decreases. Therefore, by comparing the number of signals and the distribution of the mass derived from MALDI/TOF analysis of the peptide mixture after endoproteinase Asp–N digestion, these chemical modifications can be selectively detected. To improve accuracy when determining the modified site, I performed

mass spectrometry in the presence of the corresponding stable isotope–labeled protein [63]. By this treatment, at Asn deamidate site, it becomes easy to determine the signals derived from peptide mapping with those of the corresponding labeled peptide, because I am able to obtain information concerning the difference in the mass between the sample and labeled protein signals.

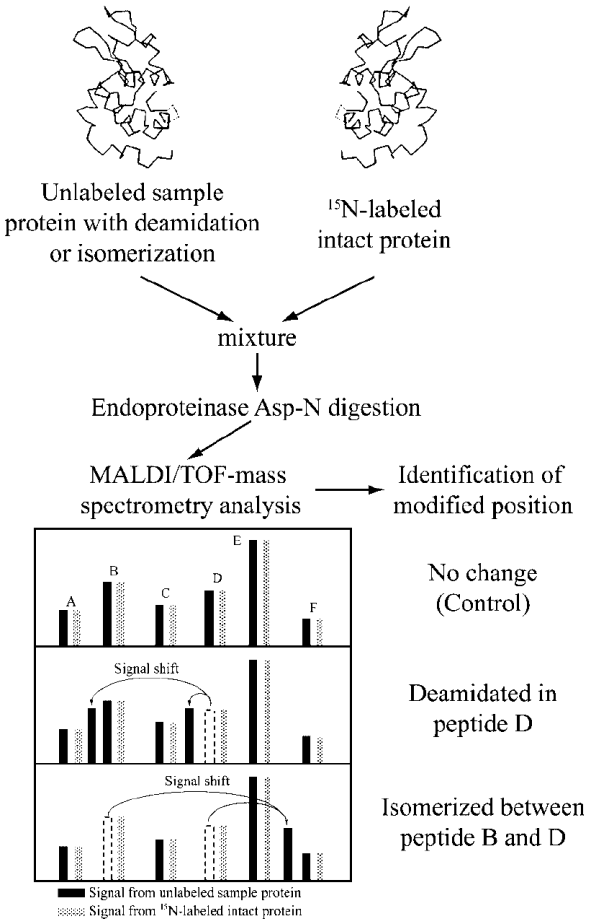

Fig. IV–1 Outline for identifying position of deamidation and isomerization in sample protein, using endoproteinase Asp–N digestion, ^{15}N–labeled intact protein and MALDI/TOF–mass spectrometry.

Therefore, I used hen egg–white lysozyme as a model protein for feasibility evaluation, because its chemical characterization has already been investigated in detail [41 ,44, 60]. I tested the validity of this method by identifying the mutated site in two mutants where Asn is mutated to Asp. Furthermore, I attempted to determine the position of deamidation or isomerization, which was reported to occur in lysozyme incubated in phosphate (pH 8.0) or acetate (pH 4.0) buffer.

Materials and Methods

Materials

Five–times–recrystallized hen egg–white lysozyme was donated by QP Company (Tokyo, Japan). Mutant lysozymes in which Asn27 and Asn44 are mutated to Asp (N27D and N44D), respectively, and ^{15}N uniformly labeled lysozyme were previously prepared in Imoto's laboratory in Graduate School of Pharmaceutical Sciences of Kyushu University [64, 65]. Resource S (1 mL) and TSK–gel ODS–120T (4.6 × 250 mm) columns were obtained from Amersham Biosciences (Piscataway, NJ, USA) and Tosoh (Tokyo, Japan), respectively. Endoproteinase Asp–N was purchased from Takara Bio (Otsu, Japan). All other chemicals used were of the highest quality commercially available.

Preparation of chemically modified lysozymes

Deamidated or isomerized lysozyme was prepared as described below. Lysozyme solution was incubated at 40°C for 7 days in 50 mM phosphate buffer (pH 8.0) for deamidation or at 60°C for 3 days in 50 mM acetate buffer (pH 4.0) for isomerization. Each modified lysozyme was purified by cation–exchange chromatography using the Resource S column (1 mL), which was eluted with a linear gradient of 30 mL of 0.05 M acetate buffer and 30 mL of the same buffer containing 0.5 M NaCl at pH 5, at a flow rate of 1 mL/min. The eluted solution of deteriorated lysozyme was dialyzed against purified water.

Reduction and S*–carboxymethylation of lysozymes*

Fifty nanomols of hen egg–white lysozyme, mutant lysozymes (N27D and N44D), chemically modified lysozyme (deamidated and racemized), and ^{15}N–labeled lysozyme were lyophilized and

dissolved in 60 µL of 0.5 M Tris–HCl buffer (pH 8.1) containing 8 M guanidine hydrochloride and 2 mM ethylenediaminetetraacetic acid (EDTA). After that, 20 µL of 2–mercaptoethanol was added to each solution, and the mixture was heated at 40°C for 2 h. Then 76 mg of iodoacetic acid sodium salt was added, and the mixture was kept in the dark for 15 min. The samples were dialyzed against 10% acetic acid solution at 4°C and then lyophilized.

Proteolytic digestion of lysozyme samples

Each *S*–carboxymethylated lysozyme (50 nmol) was dissolved in 50 µL of water. To each solution, the same amount of carboxymethylated ^{15}N–labeled lysozyme solution (50 µL) was added. Endoproteinase Asp–N digestion of the lysozyme mixtures (total: 100 nmol) was performed under the following conditions: a 100:1 weight ratio of substrate to enzyme was incubated in 200 µL of 200 mM ammonium bicarbonate buffer (pH 8.4) at 37°C for 15 h.

MALDI/TOF–Mass Spectrometry

Endoproteinase Asp–N–digested samples were analyzed on a Voyager Elite mass spectrometer (PerSeptive Biosystems) using α–cyano 4–hydroxycinnamic acid as the matrix. Each peak of the mass spectrum was identified by the mass and the difference in the mass between the unlabeled sample and the corresponding ^{15}N–labeled lysozyme. Internal calibration of molecular mass was achieved by use of a standard curve derived from peptides of the ^{15}N–labeled lysozyme. The theoretical mass of the peptides generated by endoproteinase Asp–N digestion was calculated using "PeptideMass" programs [66].

Results

Degree in separation between "unlabeled" and "^{15}N–labeled" peptides after the digestion with endoproteinase Asp–N

An equimolar mixture of "unlabeled" and "^{15}N–labeled" lysozymes was digested with endoproteinase Asp–N, and the mass of the digested mixture was measured by MALDI/TOF–mass spectrometry (Fig. IV–2). Generally, if nitrogen atoms in a protein are labeled with the ^{15}N isotope, the mass of an amino acid residue containing ^{15}N increases by 1–4 Da. The mass per amino acid residue increases by 4 Da for Arg; 3 Da for His; 2 Da for Lys, Trp, Gln, and Asn; and 1 Da for the other amino acid residues. Therefore, in this chapter, the peptides released by digestion with endoproteinase Asp–N from unlabeled and ^{15}N–labeled lysozymes, each gave a pair of peaks on MALDI/TOF–mass spectrum, depending on its each primary structure; this phenomenon indicated the coexistence of peptides with subtle differences in the mass. I compared the masses of respective pairs of peaks from unlabeled and ^{15}N–labeled peptides digested by endoproteinase Asp–N, and this information allowed the calibration of the theoretical mass (Table IV–1).

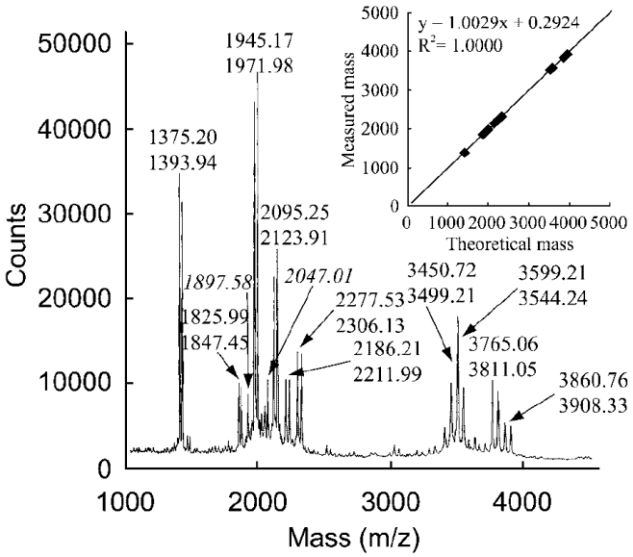

Fig. IV–2 MALDI/TOF–mass spectrum of the mixture of unlabeled lysozyme and ^{15}N–labeled lysozyme after endoproteinase Asp–N digestion. (Inset) Calibration curve of the theoretical mass from the measured mass.

Table IV–1 Expected and observed masses of peptides obtained from endoproteinase Asp–N cleavage of unlabeled and ^{15}N–labeled, carboxymethylated lysozyme, on MALDI/TOF–mass spectrometry.

Asp–N peptide	Sequence	Expected mass (m/z)			Observed mass (m/z)		
		Hen egg lysozyme	^{15}N–labeled lysozyme	Difference	Hen egg lysozyme	^{15}N–labeled lysozyme	Difference
Peptides obtained from complete cleavage of Asp–N							
1–17	KVFGRCELAAAMKRHGL	1945.03	1972.03	27.00	1945.17	1971.98	26.81
18–47	DNYRGYSLGNWVCAAKFESNFNTQATNRNT	3499.57	3544.57	45.00	3499.21	3544.24	45.03
48–51	DGST	379.15	383.15	4.00	—	—	—
52–65	DYGILQINSRWWCN	1825.83	1847.83	22.00	1825.99	1847.45	21.46
66–86	DGRTPGSRNLCNIPCSALLSS	2277.06	2306.06	29.00	2277.53	2306.13	28.60
87–100	DITASVNCAKKIVS	1506.78	1523.78	17.00	—	—	—
101–118	DGNGMNAWVAWRNRCKGT	2093.94	2123.94	30.00	2095.25	2123.91	28.66
119–129	DVQAWIRGCRL	1374.70	1393.70	19.00	1375.20	1393.94	18.74
Peptides obtained from incomplete cleavage of Asp–N							
18–51	DNYRGYSLGNWVCAAKFESNFNTQATNRNTDGST	3859.70	3908.70	49.00	3860.76	3908.33	47.57
48–65	DGSTDYGILQINSRWWCN	2185.96	2211.96	26.00	2186.21	2211.99	25.77
66–100	DGRTPGSRNLCNIPCSALLSSDITASVNCAKKIVS	3764.83	3810.83	46.00	3765.06	3811.05	45.99
101–129	DGNGMNAWVAWRNRCKGTDVQAWIRGCRL	3449.62	3498.62	49.00	3450.72	3499.21	48.49

Although six pairs of peptides were successfully identified, peptides 48–51 and 87–100 could not be identified. Since peptide 48–51 was small, consisting of only 4 amino acid residues, it was difficult to identify using MALDI/TOF–mass spectrometry. On the other hand, peptide 87–100 consisted of 14 amino acid residues, which was a sufficient mass for detection on MALDI/TOF–mass spectrometry. To determine why this peptide could not be identified, I analyzed all peptide peaks derived from endoproteinase Asp–N digests of lysozyme, which were separated on reverse–phase HPLC, using MALDI/TOF–mass spectrometry. As a result, I detected a peak with the mass corresponding to peptide 87–100 (data not shown). In general, the ionization efficiency of peptides on MALDI/TOF–mass spectrum differs according to the sequence of amino acid residues. Therefore, it was assumed that peptide 87–100 was very difficult to ionize, and could not be detected because such a large number of peptides were ionized simultaneously. Although two peaks were seen at the masses of 1897.58 and 2047.01 on MALDI/TOF–mass spectrometry (Fig. IV–2), they were considered to be derived from the self–digestion of endoproteinase Asp–N, because there was no corresponding peptide in the digest of the lysozyme by endoproteinase Asp–N.

Detectability of deamidated Asn site using mutant and incubated sample of lysozyme

I applied this method for the detection of a deamidated site in mutant lysozymes in which Asn is mutated to Asp. In the case of the N27D lysozyme, Asn27 is mutated to Asp; three additional peaks appeared at the masses of 1045.03, 2475.30, and 2971.14, after the correction of masses using the peptides of the ^{15}N–labeled lysozyme (Fig. IV–3A). Because, Asn27 changes to Asp in this mutant, peptide 18–47 in N27D lysozyme was divided into two peptides, i.e., 18–26 and 27–47, after digestion. The theoretical masses of these two peptides were 1044.47 and 2475.10, respectively. Therefore, these additional peaks (1045.03, 2475.30, and 2971.14) were assigned to peptides 18–26,

27–47, and 1–26, respectively (Table IV–2A). This result suggests that endoproteinase Asp–N was cleaved at the N–terminus of the 27th residue in the N27D lysozyme. On the other hand, in the case of the N44D lysozyme, Asn44 is mutated to Asp; two additional peaks appeared at the masses of 2672.59 and 3014.91, after the correction of masses using the peptides of the ^{15}N–labeled lysozyme (Fig. IV–3B). Because Asn44 changes to Asp in this mutant, the peptide 18–47 in N44D was divided into two peptides, 18–43 and 44–47, after digestion, and their theoretical masses were 3014.34 and 505.24, respectively. Therefore, I assigned these additional peaks with the masses at 2672.59 and 3014.91 to peptides 44–65 and 18–43, respectively (Table IV–2B). This result suggests that endoproteinase Asp–N was cleaved at the N–terminus of the 44th residue in the N44D lysozyme. It was concluded that the present method could be applied for the detection of the deamidation site of Asn in proteins.

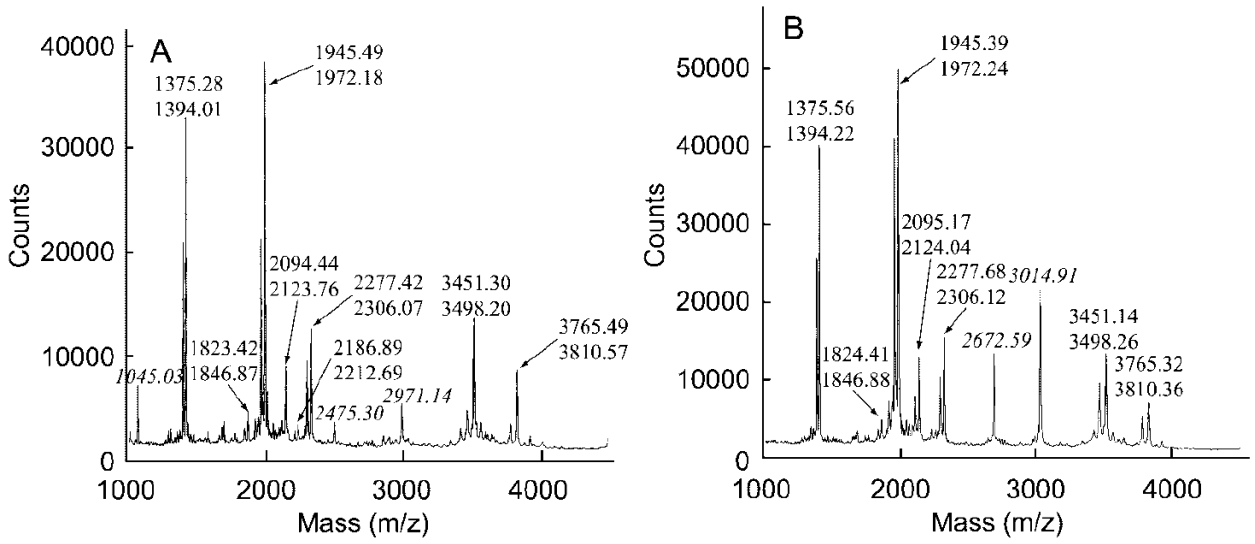

Fig. IV–3 MALDI/TOF–mass spectra of the mixtures of mutant lysozyme and ^{15}N–labeled lysozyme after endoproteinase Asp–N digestion. A, Mixture of N27D lysozyme and ^{15}N–labeled lysozyme; B, mixture of N44D lysozyme and ^{15}N–labeled lysozyme.

Table IV–2 Assignment of peaks on MALDI/TOF–mass spectrometry derived from the digests of mutant lysozyme with endoproteinase Asp–N. The correct masses were achieved by the calibration curve of peptides derived from the ^{15}N–labeled lysozyme

(A) N27D

Disappeared peptide

Asp–N peptide	Sequence	Expected mass (m/z)			Observed mass (m/z)		
		Hen egg lysozyme	^{15}N–labeled lysozyme	Difference	N27D	^{15}N–labeled lysozyme	Difference
18–47	DNYRGYSLGNWVCAAKFESNFNTQATNRNT	3499.57	3544.57	45.00	—	3545.01	—

Appeared peptides

Asp–N peptide	Corresponding peptide		Observed mass (m/z)
	Assigned sequence	Expected mass (m/z)	
18–26	DNYRGYSLG	1044.47	1045.03
27‑47	DWVCAAKFESNFNTQATNRNT	2475.10	2475.30

Table IV–2 (Continued)

(B) N44D

Disappeared peptide

Asp–N peptide	Sequence	Expected mass (m/z)			Observed mass (m/z)		
		Hen egg lysozyme	^{15}N–labeled lysozyme	Difference	N44D	^{15}N–labeled lysozyme	Difference
18–47	DNYRGYSLGNWVCAAKFESNFNTQATNRNT	3499.57	3544.57	45.00	—	3545.06	—

Appeared peptide

Asp–N peptide	Corresponding peptide		Observed mass (m/z)
	Assigned sequence	Expected mass (m/z)	
44–65	DRNTDGSTDYGILQINSRWWCN	2672.18	2672.59

The Asn and Asp residues differ in mass by only 1 Da. To detect this difference, advanced technique and sophisticated equipment are both required. Using the present method, it was determined that a new site of cleavage by endoproteinase Asp–N appears when the Asn residue changes to Asp. Therefore, the number and the mass of peptides observed on MALDI/TOF–mass spectrometry will change. The present method is thus useful for determining the deamidation site in a protein.

Generally, deamidation at the Asn residue in a protein occurs easily at basic pH [44]. I obtained an unknown peak that was eluted earlier than the intact lysozyme peak on cation–exchange HPLC after incubating the lysozyme at 40°C for 7 days in 50 mM phosphate buffer, pH 8.0 (Fig. IV–4A). MALDI/TOF–mass spectrometry analysis of endoproteinase Asp–N digests of the unknown peak, which was isolated by cation–exchange HPLC, was performed. Fig. IV–5A shows that the expected peak at the mass of 2093.94 corresponding to peptide 101–118 disappeared, and that new peaks appeared at the masses of 1897.29 and 1924.79. It was found that the peak at the mass of 1924.79 was equivalent to the position of 103–118, as determined by fitting the primary structure of the lysozyme to the mass of this peak (Table IV–3A). This suggested that peptide 101–118 was cleaved by endoproteinase Asp–N at the N–terminus of the 103rd residue in the lysozyme, because Asn103 changed to Asp during incubation. In addition, the peak at the mass of 1897.29 may be considered as the product resulting from self–digestion of endoproteinase Asp–N.

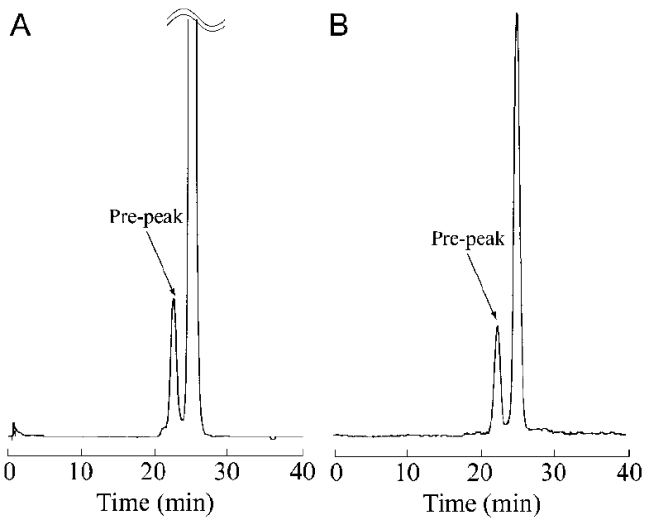

Fig. IV–4 Cation–exchange HPLC of the incubated lysozyme on Resource S (1 mL) column. The column was eluted with a linear gradient of 30 mL of 0.05 M acetate buffer and 30 mL of the same buffer containing 0.5 M NaCl at pH 5, at the flow rate of 1 mL/min. A, After incubation at 40°C for 7 days in 50 mM phosphate buffer (pH 8.0); B, after incubation at 60°C for 3 days in 50 mM acetate buffer (pH 4.0).

Detectability of isomerized Asp site using incubated sample of lysozyme

On the other hand, isomerization at the Asp residue in a protein is reported to occur at acidic pH [41]. I obtained an unknown peak that was eluted earlier than the unchanged lysozyme peak on cation–exchange HPLC after incubating the lysozyme at 60°C for 3 days in 50 mM acetate buffer, pH 4.0 (Fig. IV–4B). MALDI/TOF–mass spectrometry analysis of endoproteinase Asp–N digests of the unknown peak was performed. Fig. IV–5B shows that the expected peak at the mass of 2093.94 corresponding to peptide 101–118 disappeared, and that the new peak appeared at the mass of 3582.85, which corresponded to peptide 87–118, as determined by fitting the primary structure of the lysozyme to the mass of this peak (Table IV–3B). The results indicate that a chemical modification occurred at Asp101 in the lysozyme, and that peptide 101–118 could not be cleaved by endoproteinase Asp–N. Therefore, I concluded that Asp101 in the lysozyme had isomerized during incubation.

Table IV–3 Assignment of peaks on MALDI/TOF–mass spectrometry derived from the digests of chemically modified lysozyme with endoproteinase Asp–N. The correct masses were achieved by the calibration curve of peptides derived from the ^{15}N–labeled lysozyme

(A) Incubation in 50 mM phosphate buffer (pH8.0)

Disappeared peptide

Asp–N peptide	Sequence	Expected mass (m/z)			Observed mass (m/z)		
		Hen egg lysozyme	^{15}N–labeled lysozyme	Difference	Hen egg lysozyme	^{15}N–labeled lysozyme	Difference
101–118	DGNGMNAWVAWRNRCKGT	2093.94	2123.94	30.00	—	2122.23	—

Appeared peptide

Asp–N peptide	Corresponding peptide		Observed mass (m/z)
	Assigned sequence	Expected mass (m/z)	
103–118	DGMNAWVAWRNRCKGT	1922.88	1924.79

Table IV–3 (Continued)

(B) Incubation in 50 mM acetate buffer (pH4.0)

Disappeared peptide

Asp–N peptide	Sequence	Expected mass (m/z)			Observed mass (m/z)		
		Hen egg lysozyme	^{15}N–labeled Lysozyme	Difference	Hen egg lysozyme	^{15}N–labeled Lysozyme	Difference
101–118	DGNGMNAWVAWRNRCKGT	2093.94	2123.94	30.00	—	2123.39	—

Appeared peptide

Asp–N peptide	Corresponding peptide		Observed mass (m/z)
	Assigned sequence	Expected mass (m/z)	
87–118	DITASVNCAKKIVSDGNGMNAWVAWRNRCKGT	3581.71	3582.85

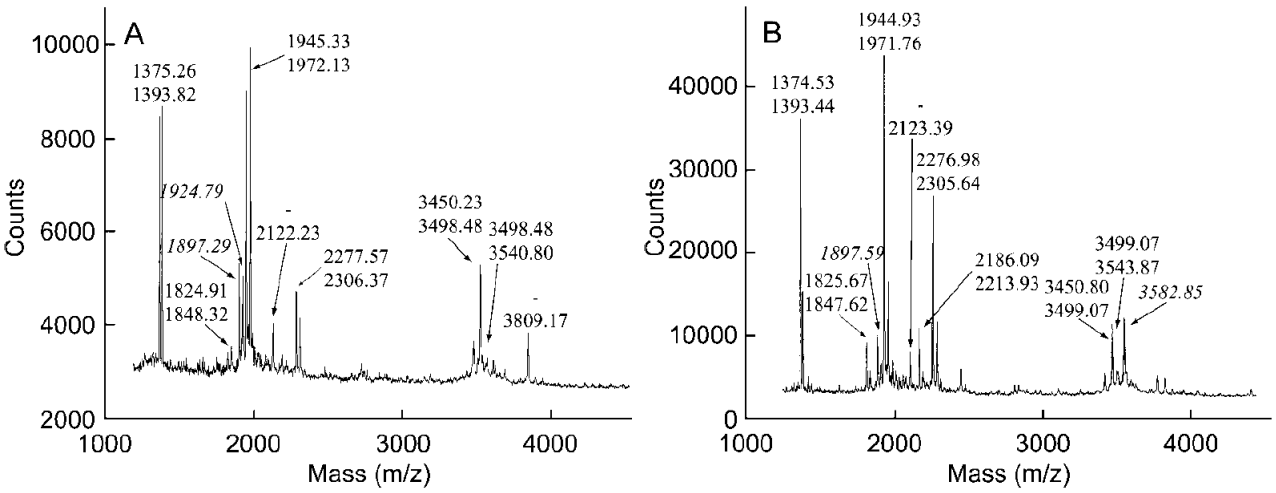

Fig. IV–5 MALDI/TOF–mass spectra of the mixtures of chemically modified lysozyme and ^{15}N–labeled lysozyme after endoproteinase Asp–N digestion. A, Mixture of the pre–peak in Fig. IV–4A and ^{15}N–labeled lysozyme; B, mixture of the pre–peak in Fig. IV–4B and ^{15}N–labeled lysozyme.

Discussion

As described above, the present method made it possible to identify the sites of deamidation of the Asn residue or isomerization of the Asp residue in the lysozyme. Therefore, this method has proven useful for identifying deamidation of the Asn residue and isomerization of the Asp residue, which has been difficult to determine by conventional methods. However, when the Asp residue produced by deamidation of the Asn residue is itself isomerized, it remains difficult to detect the change by this method, and in such a case, Edman degradation would be useful, as it analyzes the peptide sequence [67]. In this method, on the other hand, ^{15}N–labeled protein was used as a means to identify the signals and calibrate the mass of signals. However, when applying this method to proteins of high molecular weight, the signals in the MALDI/TOF–mass spectrum are complex, and it is difficult to identify each signal with the corresponding theoretical peptides. Moreover, the application of ^{15}N–labeled protein is limited to proteins that have been cloned and expressed.

However, these problems are solvable by calibrating the mass using standard peptides of known molecular weight.

This result obtained here introduced a novel method for identifying the sites of deamidation of the Asn residue or the isomerization of the Asp residue in hen egg–white lysozyme, which was used as a model protein. In the case of a protein of low molecular weight, such as a lysozyme, identification of a modified site is possible without using the present method by using reverse–phase HPLC for peptide mapping following endoproteinase Asp–N digestion. However, in the case of proteins of high molecular weight, it is generally difficult to perform peptide mapping of good quality, and therefore the present method may be beneficial for identifying modified sites. Moreover, it is expected that the application of liquid chromatography and mass spectrometry combined with this method will improve the capability of detection [68]. Recently, the method developed here was shown to be applicable to detect the deamidation of Asn residue in humanized Fab [69]. From this paper, typical mass spectrum of heated Fab (100°C for 1h) sample was obtained (Fig. IV–6), and the deamidation at Asn138 in the L–chain of the present humanized Fab was able to be detected. In this case, control of ^{15}N labeled sample was important to evaluate the signal decrease of peptide 123–151 of the L–chain of humanized Fab. Therefore, I confirmed the significance of the combination of ^{15}N isotope labeling protein and endoproteinase Asp–N digestion for improving the efficiency of detection of Asn deamidation, by peptide mapping.

Degradation of mAbs including Asn deamidation and Asp isomerization is a critical quality attribute that needs to be monitored to assess the purity and integrity of the protein. Degradation can occur during protein production in the cell culture, and is modulated by the purification process and accrues during storage. In fact, I have shown in Chapter III that some chemical modification is detected in humanized IgG under certain solution conditions. Therefore, characterization of chemical modification is indispensable for those mAbs that are developed as pharmaceuticals. For

the characterization of deamidation and isomerization of humanized IgG, the method established in this chapter will be useful for specifying the sites of these chemical modifications.

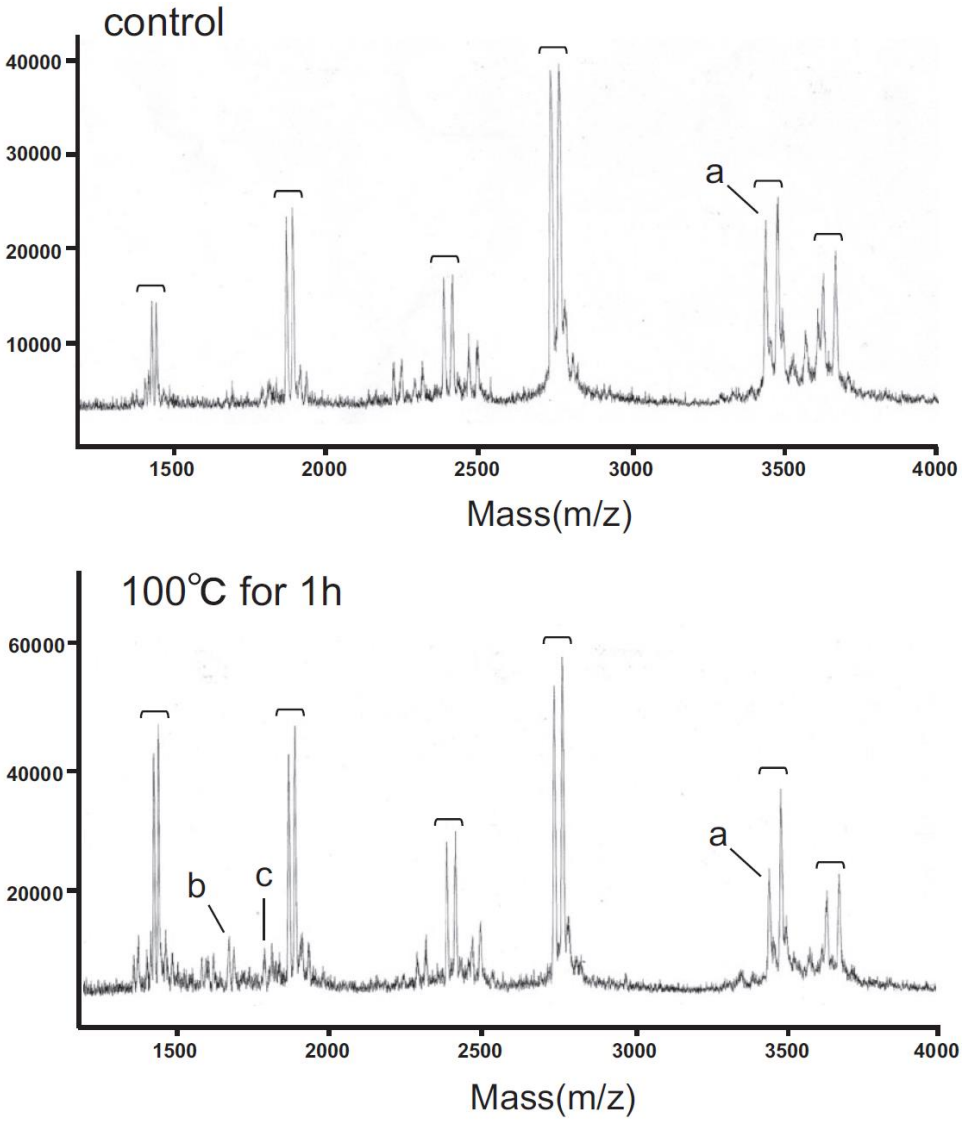

Fig. IV–6 MALDI/TOF–mass spectrum of the mixture of unlabeled L–chain and ^{15}N labelled L–chain after endoproteinase Asp–N digestion. The signal pattern derived from heated Fab (100°C for 1 h) was compared with that derived from non–heated Fab (control).

(This figure was quoted from Ohkuri, T., *et. al.* (2013) *J. Biochem.* **154,** 337.)

CONCLUSION

I performed a series of studies to understand the aggregation and the chemical modification of humanized IgG in solution from the viewpoint of developing a method to control deterioration during storage, which has become an important issue in the commercialization of antibody drug products. I clarified the effect of specific buffer species such as MES and imidazole in controlling aggregation by evaluating the influence of the buffer species on the aggregation and chemical modification of humanized IgG after heat treatment at 60°C and 80°C. That finding showed that the specific interaction between buffer molecules and the Fc region of humanized IgG significantly contributed to the effect of buffer species on the aggregation of humanized IgG (Chapter I). Evaluation of the effect of solution pH on the stability of humanized IgG in two buffer species having different effects on stability showed that the pH profiles with respect to stability of humanized IgG were not similar under different heat treatment conditions. Therefore, I clarified the contribution of structural stability on the aggregation of humanized IgG using spectroscopy and thermodynamic techniques (Chapter II). Moreover, I showed the existence of a cleavage reaction between the Asp–Pro peptide bond on the C_H2 domain as a type of chemical modification of humanized IgG that occurs under acidic conditions and the structural stability of the C_H2 domain also contributed to retarding the cleavage rate of the Asp–Pro bond (Chapter III). Finally, I established a novel analytical method using MALDI/TOF–mass spectrometry with endoproteinase Asp–N digestion for detecting Asn deamidation and Asp isomerization, which are critical types of deterioration in pharmaceutical proteins, but which are difficult to evaluate. This method was shown to apply for the evaluation of humanized Fab (Chapter IV). These results indicate the importance of considering structural stability when investigating the solution conditions designed to reduce the deterioration of humanized IgG during storage. In addition, it was shown that specific evaluations of deterioration reactions are indispensable for assuring the quality of humanized IgG during storage.

My findings would contribute to better understanding satisfactory conditions for inhibiting aggregation and chemical modification of humanized IgG during storage in solution. Therefore, I am sure that these novel findings will establish a more effective approach to finding conditions resulting in minimum deterioration during long–term storage in solution which will contribute to the development of humanized IgG as pharmaceuticals.

REFERENCES

1. Strohl, W.R. (2014) Antibody discovery: sourcing of monoclonal antibody variable domains. *Curr. Drug Discov. Technol.* **11,** 3–19
2. Lonberg, N. (2008) Fully human antibodies from transgenic mouse and phage display platforms. *Curr. Opin. Immunol.* **20,** 450–459
3. Shire, S.J. (2009) Formulation and manufacturability of biologics. *Curr. Opin. Biotech*. **20,** 708–71
4. Vázquez–Rey, M. and Lang, D.A. (2011) Aggregates in monoclonal antibody manufacturing processes. *Biotechnol. Bioeng.* **108,** 1494–1508.
5. Chen, B., Arakawa, T., Hsu, E., Narhi, L.O., Tressel, T.J., and Chien, S.L. (1994) Strategies to suppress aggregation of recombinant keratinocyte growth factor during liquid formulation development. *J. Pharm. Sci.* **83,** 1657–1661
6. Roberts, C.J., Darrington, R.T., and Whitley, M.B. (2003) Irreversible aggregation of recombinant bovine granulocyte–colony stimulating factor (bG–CSF) and implications for predicting protein shelf life. *J. Pharm. Sci.* **92,** 1095–1111
7. Townsend, M.W. and DeLuca, P.P. (1990) Stability of ribonuclease A in solution and the freeze–dried state. *J. Pharm. Sci.* **79,** 1083–1086
8. Fatouros, A., Österberg, T., and Mikaelsson, M. (1997) Recombinant factor VIII SQ–influence of oxygen, metal ions, pH and ionic strength on its stability in aqueous solution. *Int. J. Pharm.* **155,** 121–131
9. Vermeer, A.W.P. and Norde, W. (2000) The thermal stability of immunoglobulin: unfolding and aggregation of a multi–domain protein. *Biophys. J.* **78,** 394–404
10. Tischenko, V.M., Zav'yalov, V.P., Medgyesi, G.A., Potekhin, S.A., and Privalov, P.L. (1982) A Thermodynamic study of cooperative structures in rabbit immunoglobulin G. *Eur. J. Biochem.* **126,** 517–521

11. Ejima, D., Tsumoto, K., Fukada, H., Yumioka, R., Nagase, K., Arakawa, T., and Philo, J.S. (2007) Effects of acid exposure on the conformation, stability, and aggregation of monoclonal antibodies. *Proteins* **66,** 954–962
12. Laemmli, U.K. (1970) Cleavage of structural proteins during the assembly of the head of bacteriophage T4. *Nature* **227,** 680–685
13. Fink, A.L. (1998) Protein aggregation: folding aggregates, inclusion bodies and amyloid. *Fold. Des.* **3,** R9–R23
14. Chen, B., Bautista, R., Yu, K., Zapata, G.A., Mulkerrin, M.G., and Chamow, S.M. (2003) Influence of histidine on the stability and physical properties of a fully human antibody in aqueous and solid forms. *Pharm. Res.* **20,** 1952–1960
15. Raibekas, A.A., Bures, E.J., Siska, C.C., Kohno, T., Latypov, R.F., and Kerwin, B.A. (2005) Anion binding and controlled aggregation of human interleukin–1 receptor antagonist. *Biochemistry* **44,** 9871–9879
16. Vermeer, A.W.P., Norde, W., and Amerongen, A.V. (2000) The unfolding/denaturation of immunogammaglobulin of isotype 2b and its F–ab and F–c fragments. *Biophys J.* **79,** 2150–2154
17. Welfle, K., Misselwitz, R., Hausdorf, G., Höhne, W., and Welfle, H. (1999) Conformation, pH–induced conformational changes, and thermal unfolding of anti–p24 (HIV–1) monoclonal antibody CB4–1 and its Fab and Fc fragments. *Biochim. Biophys. Acta* **1431,** 120–131
18. Arakawa, T. and Timasheff, S.N. (1982) Stabilization of protein structure by sugars. *Biochemistry* **21,** 6536–6544
19. Tsumoto, K., Umetsu, M., Kumagai, I., Ejima, D., Philo, J.S., and Arakawa, T. (2004) Role of arginine in protein refolding, solubilization, and purification. *Biotechnol. Prog.* **20,** 1301–1308
20. Arakawa, T., Kita, Y., Ejima, D., Tsumoto, K., and Fukada, H. (2006) Aggregation suppression of proteins by arginine during thermal unfolding. *Protein Pept. Lett.* **13,** 921–927

21. Liu, H., Chumsae, C., Gaza–Bulseco, G., and Goedken, E.R. (2010) Domain–level stability of an antibody monitored by reduction, differential alkylation, and mass spectrometry analysis. *Anal. Biochem.* **400,** 244–250

22. Gong, R., Vu, B.K., Feng, Y., Prieto, D.A., Dyba, M.A., Walsh, J.D., Prabakaran, P., Veenstra, T.D., Tarasov, S.G., Ishima, R., and Dimitrov, D.S. (2009) Engineered human antibody constant domains with increased stability. *J. Biol. Chem.* **284,** 14203–14210

23. Van Buren, N., Rehder, D., Gadgil, H., Matsumura, M., and Jacob, J. (2009) Elucidation of two major aggregation pathways in an IgG2 antibody. *J. Pharm. Sci.* **98,** 3013–3030

24. Zheng, J.Y. and Janis, L.J. (2006) Influence of pH, buffer species, and storage temperature on physicochemical stability of a humanized monoclonal antibody LA298. *Int. J. Pharm.* **308,** 46–51

25. Perico, N., Purtell, J., Dillon, T.M., and Ricci, M.S. (2009) Conformational implications of an inversed pH–dependent antibody aggregation. *J. Pharm. Sci.* **98,** 3031–3042

26. Long, D. and Yang, D. (2009) Buffer interference with protein dynamics: A case study on human liver fatty acid binding protein. *Biophys. J.* **96,** 1482–1488

27. van Beers, M.M., Sauerborn, M., Gilli, F., Brinks, V., Schellekens, H., and Jiskoot, W. (2011) Oxidized and aggregated recombinant human interferon beta is immunogenic in human interferon beta transgenic mice. *Pharm. Res.* **28,** 2393–2402

28. Moss, C.X., Matthews, S.P., Lamont, D.J., and Watts, C. (2005) Asparagine deamidation perturbs antigen presentation on class II major histocompatibility complex molecules. *J. Biol. Chem.* **280,** 18498–18503

29. Wakankar, A.A., Borchardt, R.T., Eigenbrot, C., Shia, S., Wang, Y.J., Shire, S.J., and Liu, J.L. (2007) Aspartate isomerization in the complementarity–determining regions of two closely related monoclonal antibodies. *Biochemistry* **46**, 1534–1544

30. Teshima, G., Porter, J., Yim, K., Ling, V., and Guzzetta, A. (1991) Deamidation of soluble CD4 at asparagine–52 results in reduced binding capacity for the HIV–1 envelope glycoprotein gp120. *Biochemistry* **30**, 3916–3922

31. Datta–Mannan, A., Witcher, D.R., Tang, Y., Watkins, J., and Wroblewski, V.J. (2007) Monoclonal antibody clearance. Impact of modulating the interaction of IgG with the neonatal Fc receptor. *J. Biol. Chem.* **282**, 1709–1717

32. Reubsaet, J.L., Beijnen, J.H., Bult, A., van Maanen, R.J., Marchal, J.A., and Underberg, W.J. (1998) Analytical techniques used to study the degradation of proteins and peptides: chemical instability. *J. Pharm. Biomed. Anal.* **17,** 955–978.

33. Geiger, T. and Clarke, S. (1987) Deamidation, isomerization, and racemization at asparaginyl and aspartyl residues in peptides. Succinimide–linked reactions that contribute to protein degradation. *J. Biol. Chem.* **262**, 785–794

34. Tyler–Cross, R. and Schirch, V. (1991) Effects of amino acid sequence, buffers, and ionic strength on the rate and mechanism of deamidation of asparagine residues in small peptides *J. Biol. Chem.* **266**, 22549–22556

35. Huang, L., Lu, J., Wroblewski, V.J., Beals, J.M., and Riggin, R.M. (2005) In vivo deamidation characterization of monoclonal antibody by LC/MS/MS. *Anal. Chem.* **77,** 1432–1439

36. de Laureto, P.P., de Filippis, V., Scalamella, E, Zambonin, M., and Fontana, A. (1995) Limited proteolysis of lysozyme in trifluoroethanol. Isolation and characterization of a partially active enzyme derivative. *Eur. J. Biochem.* **230,** 779–787

37. .Manning, M.C., Chou, D.K., Murphy, B.M., Payne, R.W., and Katayama, D.S. (2010) Stability of protein pharmaceuticals: an update. *Pharm. Res.* **27,** 544–575

38. Lidell, M.E., Johansson, M.E., and Hansson, G.C. (2003) An autocatalytic cleavage in the C terminus of the human MUC2 mucin occurs at the low pH of the late secretory pathway. *J. Biol. Chem.* **278**, 13944–13951

39. Landon, M. (1977) Limited proteolysis of lysozyme in trifluoroethanol. Isolation and characterization of a partially active enzyme derivative. *Methods Enzymol.* **47**, 145–149

40. Tischenco, V.M., Abramov, V.M., and Zav'yalov V.P. (1998) Investigation of the cooperative structure of Fc fragments from myeloma immunoglobulin G. *Biochemistry* **37**, 5576–5581

41. Tomizawa, H., Yamada, H., and Imoto, T. (1994) Stabilization of lysozyme against irreversible inactivation by alterations of the Asp–Gly sequences. *Biochemistry* **33**, 13032–13037

42. Ueda, T., Nagata, M., and Imoto, T. (2001) Aggregation and chemical reaction in hen lysozyme caused by heating at pH 6 are depressed by osmolytes, sucrose and trehalose. *J. Biochem.* **130**, 491–496

43. Xie, M., Shahrokh, Z., Kadkhodayan, M., Henzel, W.J., Powell, M.F., Borchardt, R.T., and Schowen, R.L. (2003) Asparagine deamidation in recombinant human lymphotoxin: hindrance by three–dimensional structures. *J. Pharm. Sci.* **92**, 869–880

44. Moudgil, K.D. and Sercarz, E.E. (1993) Dominant determinants in hen eggwhite lysozyme correspond to the cryptic determinants within its self–homologue, mouse lysozyme: implications in shaping of the T cell repertoire and autoimmunity. *J. Exp. Med.* **178,** 2131–2138

45. Ahern, T.J. and Klibanov, A.M. (1985) The mechanisms of irreversible enzyme inactivation at 100ºC. *Science* **228**, 1280–1284

46. Zale, S.E. and Klibanov, A.M. (1986) Why does ribonuclease irreversibly inactivate at high temperatures? *Biochemistry* **25**, 5432–5444

47. di Salvo, M.L., Delle Fratte, S., Maras, B., Bossa, F., Wright, H.T., and Schirch, V. (1999) Deamidation of asparagine residues in a recombinant serine hydroxymethyltransferase. *Arch. Biochem. Biophys.* **372**, 271–279

48. Perkins, M., Theiler, R., Lunte, S., and Jeschke, M. (2000) Determination of the origin of charge heterogeneity in a mural monoclonal antibody. *Pharm. Res.* **17**, 1110–1117

49. Qin, K., Yang, D.S., Yang Y., Chishti, M.A., Meng, L.J., Kretzschmar, H.A., Yip, C.M., Frasser, P.E., and Westaway, D. (2000) Copper(II)–induced conformational changes and protease resistance in recombinant and cellular PrP. Effect of protein age and deamidation. *J. Biol. Chem.* **275**, 19121–19131

50. Paranandi, M.V., Guzzetta, A.W., Hancock, W.S., and Aswad, D.W. (1994) Deamidation and isoaspartate formation during in–vitro aging of recombinant tissue–plasminogen activator. *J. Biol. Chem.* **269**, 243–253

51. Watanabe, A., Takio, K., and Ihara, Y. (1999) Deamidation and isoaspartate formation in smeared tau in paired helical filaments. Unusual properties of the microtubule–binding domain of tau. *J. Biol. Chem.* **274**, 7368–7378

52. Shahrokh, Z., Eberlein, G., Buckley, D., Paranandi, M.V., Aswad, D.W., Stratton, P., Mischak, R., and Wang, Y.J. (1994) Major degradation products of basic fibroblast growth factor: detection of succinimide and iso–aspartate in place of aspartate. *Pharm. Res.* **11**, 936–944

53. Brange, J., Langkjaer, L., Havelund, S., and Volund, A. (1992) Chemical stability of insulin. 1. Hydrolytic degradation during storage of pharmaceutical preparations. *Pharm. Res.* **9**, 715–726

54. Fujii, N., Takemoto, L.J., Momose, Y., Matsumoto, S., Hiroki, K., and Akaboshi, M. (1999) Formation of four isomers at the Asp–151 residue of aged human αA–crystallin by natural aging. *Biochem. Biophys. Res. Commun.* **265**, 746–751

55. Fujii, N., Matsumoto, S., Hiroki, K., and Takemoto, L. (2001) Inversion and isomerization of Asp–58 residue in human αA–crystallin from normal aged lenses and cataractous lenses. *Biochim. Biophys. Acta* **1549**, 179–187

56. Stephenson, R.C. and Clarke, S. (1989) Succinimide formation from aspartyl and asparaginyl peptides as a model for the spontaneous degradation of proteins. *J. Biol. Chem.* **264**, 6164–6170

57. Battersby, A.R. and Robinson, J.C. (1955) Studies on specific chemical fission of peptide links. Part I. The rearrangement of aspartyl and glutamyl peptides. *J. Chem. Soc.* 259–269

58. Song, E.J., Kim, Y.S., Chung, J.Y., Kim, E., Chae, S.K., and Lee, K.J. (2000) Oxidative modification of nucleoside diphosphate kinase and its identification by matrix–assisted laser desorption/ionization time–of–flight mass spectrometry. *Biochemistry* **39**, 10090–10097

59. Griffiths, S.W. and Cooney, C.L. (2002) Development of a peptide mapping procedure to identify and quantify methionine oxidation in recombinant human α1–antitrypsin. *J. Chromatogr. A* **942**, 133–143

60. Tomizawa, H., Yamada, H., Ueda, T., and Imoto, T. (1994) Isolation and characterization of 101–Succinimide lysozyme that possesses the cyclic imide at Asp101–Gly102. *Biochemistry* **33**, 8770–8774

61. Kinzel, V., König, N., Pipkorn, R., Bossemeyer, D., and Lehmann, W.D. (2000) The amino terminus of PKA catalytic subunit—a site for introduction of posttranslational heterogeneities by deamidation: D–Asp2 and D–isoAsp2 containing isozymes. *Protein Sci.* **9**, 2269–2277

62. Noreau, J. and Drapeau, G.R. (1979) Isolation and properties of the protease from the wild–type and mutant strains of *Pseudomonas fragi*. *J. Bacteriol.* **140**, 911–916

63. Oda, Y., Huang, K., Cross, F.R., Cowburn, D., and Chait, B.T. (1999) Accurate quantitation of protein expression and site–specific phosphorylation. *Proc. Natl Acad. Sci. USA* **96**, 6591–6596

64. Tomizawa, H., Yamada, H., Hashimoto, Y., and Imoto, T. (1995) Stabilization of lysozyme against irreversible inactivation by alterations of the Asp–Gly sequences. *Protein Eng.* **8**, 1023–1028

65. Mine, S., Ueda, T., Hashimoto, Y., Tanaka, T., and Imoto, T. (1999) High–level expression of uniformly ^{15}N–labeled hen lysozyme in *Pichia pastoris* and identification of the site in hen lysozyme where phosphate ion binds using NMR measurements. *FEBS Lett.* **448**, 33–37

66. Wilkins, M.R., Lindskog I., Gasteiger, E., Bairoch, A., Sanchez, J.C., Hochstrasser, D.F., and Appel, R.D. (1997) Detailed peptide characterization using PEPTIDEMASS–a World‐Wide‐Web‐accessible tool *Electrophoresis* **18**, 403–408

67. Johnson, B.A., Shirokawa, J.M., Hancock, W.S., Spellman, M.W., Basa, L.J., and Aswad, D.W. (1989) Formation of isoaspartate at two distinct sites during in vitro aging of human growth hormone. *J. Biol. Chem.* **264**, 14262–14271

68. Mock, K., Hail, M., Mylchreest, I., Zhou, J., Johnson, K., and Jardine, I. (1993) Rapid high–sensitivity peptide mapping by liquid chromatography–mass spectrometry. *J. Chromatogr.* **646**, 169–174

69. Ohkuri, T., Murase, E., Sun, S‐L., Sugitani, L. and Ueda, T. (2013) Characterization of deamidation at Asn138 in L–chain of recombinant humanized Fab expressed from *Pichia pastoris*. *J. Biochem*. **154**, 333–340

ACKNOWLEDGEMENTS

I would like to thank Prof. T. Ueda of Graduate School of Pharmaceutical Sciences, Kyushu University, for his helpful guidance and advice during course of this work and for critical reading of this manuscript. I would like to thank Prof. K. Tsumoto of School of Engineering, The University of Tokyo, Dr. Y. Abe and Dr. K. Hamase of Graduate School of Pharmaceutical Sciences, Kyushu University, for their useful discussions and reading of this manuscript. I wish to express my special thanks to Prof. Emeritus T. Imoto of Graduate School of Pharmaceutical Sciences, Kyushu University, for helpful guidance and advice. I wish to thank my co–workers in Chugai Pharmaceutical Co. Ltd., for giving me the opportunity of this work. I wish to express my special thanks to Mr. E. Masuzaki for their experimental assistance. I thank my co–workers in Immunobiochemistry of Graduate School of Pharmaceutical Sciences, Kyushu University, for their friendship and warm supports in various directions.

PUBLISHED PAPERS

1. Kameoka, D., Masuzaki, E., Ueda, T., and Imoto, T. (2007) Effect of buffer species on the unfolding and the aggregation of humanized IgG. *J. Biochem.* **142,** 383–391
   (Corresponding to Chapter I.)
2. Kameoka, D., Ueda, T., and Imoto, T. (2011) Effect of the conformational stability of the C_H2 domain on the aggregation and peptide cleavage of a humanized IgG. *Appl. Biochem. Biotechnol.* **164,** 642–654
   (Corresponding to Chapter II and III.)
3. Kameoka, D., Ueda, T., and Imoto, T. (2003) A method for the detection of asparagine deamidation and aspartate isomerization of proteins by MALDI/TOF–mass spectrometry using endoproteinase Asp–N. *J. Biochem.* **134,** 129–135
   (Corresponding to Chapter IV.)

PUBLICATION OR APPLICATION OF PATENT

1. 中外製薬株式会社，井本泰治，植田正，亀岡大介，タンパク質製剤，特許 5052736 号，2012‐08‐03
   (Related to from Chapter I to III.)
2. 中外製薬株式会社，井本泰治，植田正，亀岡大介，タンパク質の変性度測定方法，特開 2002‐340903，2002‐11‐27
   (Related to from Chapter I to III.)